universität wien

MASTERARBEIT | MASTER'S THESIS

Titel | Title

Bounding spectral gaps in the Matrix Product State formalism

verfasst von | submitted by

Milán Ádám Rozmán BSc

angestrebter akademischer Grad | in partial fulfilment of the requirements for the degree of

Master of Science (MSc)

Wien | Vienna, 2024

Studienkennzahl lt. Studienblatt | Degree programme code as it appears on the student record sheet:	UA 066 876
Studienrichtung lt. Studienblatt | Degree programme as it appears on the student record sheet:	Masterstudium Physics
Betreut von | Supervisor:	Univ.-Prof. Dr. Norbert Schuch
Mitbetreut von | Co-Supervisor:	Dr. András Molnár master MSc

Acknowledgements

Here I would like to thank my supervisor and my co-supervisor, Prof. Norbert Schuch and Dr. András Molnár for their consistent help and the countless discussions we had throughout the writing process of the thesis and for the possibility to write this thesis in the research group of Quantum Information and Quantum Many-Body Physics. I would like to also thank Dr. Ilya Kull for his helpful remarks. I am furthermore thankful for the Vienna Doctoral School of Physics for providing me a fellowship for the academic year 2023/24.

Abstract

The aim of this thesis is to discuss and compare the two most well-utilized methods to bound and to prove the existence of the spectral gap of quantum spin systems on an infinite chain. Knabe's method provides a gap estimate based on finite-size criteria. On the other hand, the martingale method proves the existence on the spectral gap by exploiting certain properties of the ground space structure of a given system. The latter provides powerful results for systems which fit into the matrix product state (MPS) formalism. Some of those results are reformulated in a simplified, graphical notation to be more accessible without the knowledge on the mathematical study of C*-algebras. The comparison of the two methods are discussed through an analysis on the spectral gap of $\mathbb{Z}_3$- and $\mathbb{Z}_4$-symmetric clock models without an external field, which were deformed via Witten's conjugation.

Zusammenfassung

In dieser Arbeit werden die beiden am häufigsten verwendeten Methoden zur Abschätzung und zum Beweis der Existenz der spektralen Lücke von Quantenspinsystemen auf einer unendlichen Kette vorgestellt und verglichen. Die Methode von Knabe liefert eine Abschätzung der Lücke basierend auf Kriterien für endliche Systeme. Die Martingal-Methode hingegen beweist die Existenz der spektralen Lücke, indem sie bestimmte Eigenschaften des Grundzustandsraums von einem gegebenen System ausnutzt. Die letztere Methode liefert wirkungsvolle Ergebnisse für Systeme, die in das Formalismus der Matrixproduktzustände passen. Einige von diesen Ergebnissen werden in einer vereinfachten, graphischen Notation umformuliert, um sie zugänglicher zu machen, ohne dass Kenntnisse über das mathematische Umfeld von C*-Algebren erforderlich sind. Der Vergleich beider Methoden wird durch eine Analyse der spektralen Lücke von $\mathbb{Z}_3$- und $\mathbb{Z}_4$-symmetrischen Potts-Modellen ohne externes Feld, die durch Witten-Konjugation deformiert wurden, diskutiert.

Contents

1. Introduction

One of the main difficulties of quantum many-body physics is the number of parameters of a given system which increases exponentially with the particle number of the system, often leading to computationally unfeasible scenarios. Even for a small macroscopic object, it is technically impossible to conclude every nuance of its physics by solely relying on the parameters of its building blocks i.e. atoms and particles. One possible way out is to construct toy models that exhibit a range of intriguing universal phenomena, and then investigate the physical systems that showcase the phenomena. Another strategy is to restrict the analysis to wave functions which entail physically relevant properties with a controlled number of parameters necessary to describe its behavior. In this thesis, both of these strategies are utilized to obtain low-temperature properties of quantum many-body systems.

The antiferromagnetic Heisenberg model is a paradigmatic example for a quantum spin chain model that has been in the center of interest due to its universality and rich underlying physics. For the spin-1/2 chain, Bethe [1] provided the first exact solution in 1931, which was then followed by an array of advancements in quantum many-body physics, for instance the Yang-Baxter equation [2, 3]. In 1983, Haldane concluded [4, 5] that the low-energy physics of the antiferromagnetic Heisenberg model differs for systems with half-integer and integer spin quantum numbers. In particular, for integer spin systems the Hamiltonian is accompanied with a nonzero spectral gap in the thermodynamic limit, whereas for half-integer chains the system is gapless. The bound on the finite-size spectral gap of the half-integer chain was proven to be inversely proportional to the system size by the Lieb-Schultz-Mattis theorem [6][7, Thm. 6.3]. Moreover, the AKLT model [8] serves as the first spin-1 example of a quantum spin system which was proven to have [8, 9, 10] a unique ground state and a spectral gap in the thermodynamic limit, supporting Haldane's conjecture to a further extent. The ground state of this particular model belongs to the class of valence bond solid states, which was generalized by Fannes, Nachtergaele and Werner [10], giving rise to the class of C*-finitely correlated states, which consists of translation invariant quantum states, whose correlations can be depicted with a finite dimensional object, on an infinite spin chain. Under specific restrictions, one can construct a translation invariant local Hamiltonian, which has a nonzero spectral gap and a unique ground state, which is C*-finitely correlated, in the thermodynamic limit. This construction motivated the study of matrix product states [11], which generalized the C*-finitely correlated state formalism to finite and non-translation invariant systems. Furthermore, matrix product states serve as a powerful tool to approximate ground states of local gapped Hamiltonians on quantum spin chains [12]. Exact representations are also possible: for instance, the ground state of the AKLT model was also characterized as an

matrix product state [11]. The fact that the Hamiltonian of the AKLT model can be explicitly constructed by its unique ground state is related to the injectivity of the matrix product state. The notions of C*-finitely correlated states, matrix product states and injectivity will be properly defined throughout the thesis.

The relevance of the study of infinite-size systems is first motivated by an example: the antiferromagnetic Heisenberg model for a spatial dimension larger than two was proven to have a unique ground state by the Marshall-Lieb-Mattis theorem if the lattice is connected and bipartite with the sublattices having an equal number of sites [13, 14]. However, those states are not observed in experimental settings [15], which can be explained by the low-lying excitations of the finite system, which leads to an infinite number of ground states in the thermodynamic limit [7]. Consequently, taking the thermodynamic limit is often essential to properly unlock the experimentally observable physics of a quantum system.

The paradigm of gapped and gapless quantum Hamiltonians also serves as an important tool to classify quantum phases of matter: two translation invariant local gapped Hamiltonians are said to be in the same phase if they can be connected by a path of local gapped Hamiltonians [16]. This classification allows for the description of phenomena, which cannot be explained with Landau's well-established theory of phase transitions and spontaneous symmetry breaking, such as symmetry-protected topological phases [17].

The thesis is structured as follows: Chapter 2 introduces a graphical notation which allows for a simplified description of results obtained later in the thesis.

Chapter 3 focuses on the two aforementioned classes of states (matrix product states and C*-finitely correlated states), their properties and their interrelations. It also introduces the notion of injective matrix product states, for which a parent Hamiltonian can be defined.

The two most well-established methods to prove the existence of the spectral gap of frustration-free Hamiltonians are discussed in Chapter 4. Furthermore, we prove that the parent Hamiltonian of an injective matrix product state is always gapped in the thermodynamic limit, and we also provide a bound for the spectral gap. The proof is a reformulation of the results in [10] in a more accessible form via the graphical notation introduced in Chapter 2. We also discuss the extension of this argument to Hamiltonians, which have a finite number of injective matrix product ground states in the thermodynamic limit.

Chapter 5 aims to introduce Witten's conjugation for frustration-free spin chain systems based on [18], then applies it to quantum mechanical analogues of the clock model without an external field. Then, Knabe's method and the martingale method are utilized to prove the existence of the spectral gap and to provide a lower bound for them. The results are compared, and the two methods are then qualitatively contrasted.

Finally, a more elaborate discussion is provided in Chapter 6 with possible improvements and extensions of the analysis that was carried out throughout the thesis.

2. Tensor network notation

This section aims to provide the necessary building blocks for the graphical notation which is used throughout the thesis, primarily based on [19]. The orientation of the diagrams will be denoted by arrows in the first examples.

Given a complex finite-dimensional vector space V, any vector $v \in V$ will be represented as a node with one outgoing half-line which is going to be called a leg:

$$v = \text{—•} v \ \in V. \tag{2.1}$$

A linear functional $\alpha : V \to \mathbb{C}$ will correspondingly have an ingoing leg:

$$\alpha = \ \alpha \text{•—} \in V^* \tag{2.2}$$

As a consequence, we can demonstrate the action of the functional α on the vector v as

$$\alpha(v) = \ \alpha \text{•—•} v \ \in \mathbb{C}. \tag{2.3}$$

Each line between two nodes is regarded to be a summation over a single index. A simple example would be the standard scalar product on $\mathbb{C}^n$, which can be represented in the bra-ket notation as $\langle x|y\rangle = \sum_i x^i y^i$ for $x, y \in \mathbb{C}^n$, so it is exactly of the form as Eq. (2.3) in the graphical notation. The identification of a ket vector $|v\rangle$ with Eq. (2.1) and a bra vector $\langle\alpha|$ with Eq. (2.2) may also serve as a useful way to intuitively view such diagrams.

This notion can be generalized: in the graphical notation, a diagram which has no free in- or outgoing legs will be seen as a complex number, which will be especially useful for representing linear functionals on matrix spaces, for instance the trace.

A matrix M, given that it can be understood as a linear map between vector spaces, i.e. given complex vector spaces V and W, where $M \in L(V, W)$ can be represented as a node with an ingoing and an outgoing leg. For the sake of completeness, the domain and codomain of the map will be included in the graphical notation as well, but in later sections they will be omitted.

$$M = \ M \text{•} \begin{matrix} W \\ \\ V \end{matrix} \tag{2.4}$$

It is important to emphasise that a right-angle bend without a node does not correspond to any mapping. However, this notation is going to be often simplified, namely the in-

and outgoing legs will not necessarily travel through a 90 degree angle. Furthermore, if the orientation is known, it is also allowed to represent the linear map on a horizontal line. These considerations are going to be useful in some scenarios, when more complicated objects (for example higher-rank tensors) have to be represented in the graphical notation. As a consequence, we can represent $M \in L(V, W)$ as

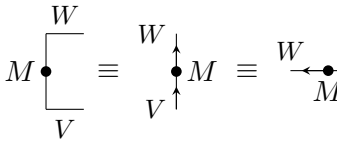

(2.5)

The identity transformation $\mathbb{1}_V$ that maps each vector $v \in V$ to itself is going to be represented without a node:

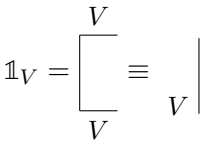

(2.6)

Tensor products of matrices are represented by drawing the lines of their respective spaces next to each other while avoiding any crossing. For $M \in L(V, W)$ and $N \in L(V', W')$ where V' and W' are also vector spaces, we have:

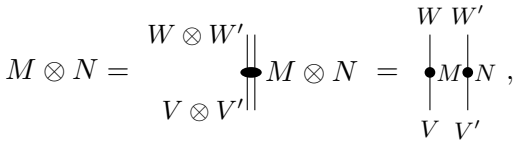

(2.7)

Tensor network notation generally refers to the graphical representation of rank-r tensors, where r is the sum of in- and outgoing legs. Scalars, vectors and matrices are thus rank-0, rank-1 and rank-2 tensors, respectively. A linear map $A : V \to W \otimes X$ between vector spaces V, W and X serves as a practical example of a higher-rank tensor. For many-body systems, where each single-particle state of the system is going to be represented by a vector in a complex finite-dimensional Hilbert space, the construction given in Eq. (2.8) provides a more illustrative way to represent the building blocks of a matrix product state which is going to be introduced in Chapter 3.

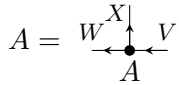

(2.8)

It is also useful to construct compositions of linear maps (especially matrix multiplication, once we fix a basis) in the tensor network notation. Given vector spaces V, W, X and linear maps $M : V \to W$ and $N : W \to X$, the composition $N \circ M$ is again a linear map, but between the spaces V and X:

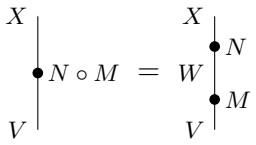

(2.9)

A linear functional ρ on a matrix space is constructed analogously to the functional on vector spaces in Eq. (2.3):

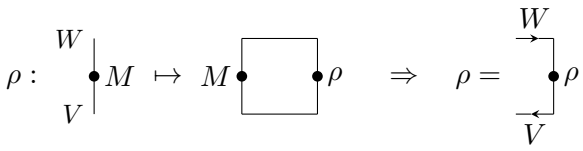

(2.10)

As shown in Eq. (2.10), ρ can be understood as a map $\rho : W \to V$. This originates from the fact that any linear functional ρ on a matrix space is of the form $\rho : M \mapsto \mathrm{Tr}(\rho M)$. A special case of such linear functionals is the trace of square matrices. Let $M \in \mathcal{M}_n(\mathbb{C})$ be an n-dimensional complex square matrix. Then its trace can be formalized by applying $\mathbb{1}$ as a linear functional:

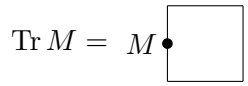

(2.11)

The graphical notation enables us to check for certain properties of the trace, for instance the cyclicity. For two square matrices M and N the proof is by moving one of the matrices through the loop in the diagram:

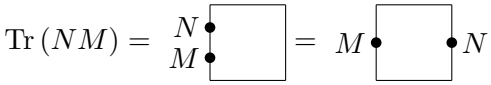

(2.12)

The key point in the graphical proof is that N is viewed as a linear functional, which is then of the form $N(M) = \mathrm{Tr}(NM)$. Similarly, we have

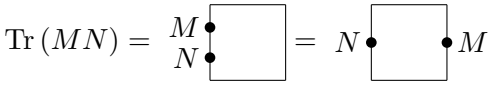

(2.13)

One can obtain the object on the right hand side of Eq. (2.12) by rotating the diagram on the right hand side of Eq. (2.13) by 180 degrees while preserving the orientation, thus the two objects are equal.

With the help of the tensor network notation it is also possible to construct more complicated linear maps between vector spaces. An example, which is going to appear in later chapters, is a linear map $X : \mathcal{M}_n(\mathbb{C}) \to \mathcal{M}_k(\mathbb{C})$, which is completely positive, thus it admits a Kraus-representation: for $M \in \mathcal{M}_n$ there exists some $V_i : \mathbb{C}^k \to \mathbb{C}^n$ such that

$$X(M) = \sum_i V_i^\dagger M V_i. \tag{2.14}$$

The equation above can be represented in the tensor network notation as:

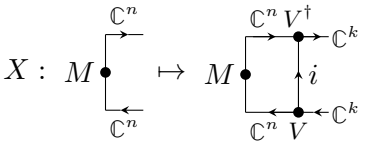

(2.15)

If X is in addition trace-preserving, meaning that $\mathrm{Tr}(X(M)) = \mathrm{Tr}(M)$, then:

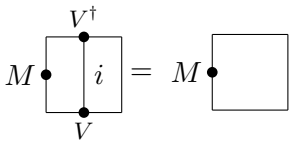

(2.16)

The notation introduced in this section should provide the most important ingredients to represent and to help to characterize matrix product states.

3. Matrix product states and C*-finitely correlated states

3.1. Matrix Product States

This section aims to introduce the most important definitions and notions of the matrix product state (MPS) formalism. The definitions, theorems and notational convention is mainly based on [11, 20, 21], unless otherwise stated.

The basic building block of the MPS construction is a tensor M, which can be understood as a linear map $\mathbb{C}^D \to \mathbb{C}^D \otimes \mathbb{C}^d$ between finite-dimensional Hilbert spaces. Let $\{|\alpha\rangle\}_{\alpha=0}^{D-1}$ and $\{|k\rangle\}_{k=0}^{d-1}$ the computational bases of $\mathbb{C}^D$ and $\mathbb{C}^d$, respectively. Then M can be written as

$$M = \sum_{\alpha,\beta,k} M^k_{\alpha\beta} |\alpha\rangle\langle\beta| \otimes |k\rangle = \quad . \tag{3.1}$$

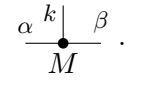

Essentially, an MPS tensor consists of d $D \times D$ matrices indexed by k and represents a d-level single-body quantum spin system. Hence, k will be called the physical index, and the dimension D of the auxiliary space will be called the bond dimension.

Now, consider a two-body spin system with physical indices k_1 and k_2, each one corresponding to a d-level quantum system. One can construct a basis by taking the tensor product of the single-spin bases $\{|k_1\rangle \otimes |k_2\rangle\}_{k_1,k_2=0}^{d-1}$. Throughout the thesis, this notation will be simplified to $|k_1\rangle \otimes |k_2\rangle = |k_1 k_2\rangle$. To represent such two-spin systems as an MPS in general, we need two tensors $M^{(1)}, M^{(2)}$ of the form given in Eq. (3.1), concatenated in the following fashion:

$$M^{(1)}M^{(2)} = \sum_{\alpha,\beta,\gamma,k_1,k_2} M^{(1),k_1}_{\alpha\beta} M^{(2),k_2}_{\beta\gamma} |\alpha\rangle\langle\gamma| \otimes |k_1 k_2\rangle = \quad , \tag{3.2}$$

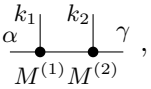

so $M^{(i)} = \sum_{k_i} M^{(i),k_i} \otimes |k_i\rangle$.

Throughout the thesis, matrix product states will be primarily used with periodic boundary conditions, namely the N-body state is represented such that we identify $N+1$ with 1. Physically, this construction means placing the N spins on a ring. A matrix product state $|\Psi\rangle$ on an N-site spin chain with periodic boundary is defined as

$$|\Psi\rangle = \sum_{k_1,\dots k_N=0}^{d} \mathrm{Tr}\left[M^{(1),k_1} M^{(2),k_2} \dots M^{(N),k_N}\right] |k_1 k_2 \dots k_N\rangle = \tag{3.3}$$

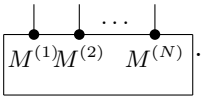

Note that any many-body quantum state can be represented by an MPS [22], but generally, the notion of MPS is restricted to states where the bond dimension does not depend on the system size N. Where this condition holds, the MPS formalism provides powerful methods to characterize the behavior of quantum systems with a large number of particles, since the system can be described with a relatively small amount of degrees of freedom. Note that the number of parameters needed to describe the state still depends on the system size N, but only in a linear fashion.

To extend the analyzability to infinite chains, i.e. for systems with $N \to \infty$, we introduce translation invariant MPS, which is defined through a single tensor M:

$$|\Psi\rangle = \sum_{k_1,\dots k_N=0}^{d} \mathrm{Tr}\left[M^{k_1} M^{k_2} \dots M^{k_N}\right] |k_1 k_2 \dots k_N\rangle = \tag{3.4}$$

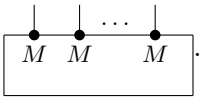

If such a representation of a state is possible, we only need $d \cdot D^2$ parameters to describe it, which provides a significant reduction in the number of parameters compared to the non-translation invariant case with periodic boundary conditions.

In some cases, it is more illustrative to block the tensors. In the translation invariant case, a tensor M' is defined to be the blocking of M if

$$M' = \sum_{k_1,\dots,k_{N'}} M^{k_1} \dots M^{k_{N'}} |k_1 \dots k_{N'}\rangle \text{ for } N'/N \in \mathbb{N}. \tag{3.5}$$

Consider the (not normalized) equal weight superposition of the spin 1/2 Néel-ordered states

$$|\Psi\rangle = |0101\dots\rangle + |1010\dots\rangle, \tag{3.6}$$

which can be represented as a translation invariant MPS with the tensors

$$M^0 = \begin{pmatrix} 0 & 1 \\ 0 & 0 \end{pmatrix}, \qquad M^1 = \begin{pmatrix} 0 & 0 \\ 1 & 0 \end{pmatrix}. \tag{3.7}$$

The construction above yields the state given in Eq. (3.6) by the definition in Eq. (3.4), since $(M^0)^2 = (M^1)^2 = 0$, so after any $|0\rangle$-state only a $|1\rangle$-state can appear with a nonzero weight. After blocking pairs of consecutive sites, we arrive at the MPS representation

$$(M')^{\tilde{0}} = \begin{pmatrix} 1 & 0 \\ 0 & 0 \end{pmatrix}, \qquad (M')^{\tilde{1}} = \begin{pmatrix} 0 & 0 \\ 0 & 1 \end{pmatrix}, \tag{3.8}$$

where we set $|\tilde{0}\rangle = |01\rangle$ and $|\tilde{1}\rangle = |10\rangle$. Eq. (3.8) is exactly the matrix product representation of the Greenberger–Horne–Zeilinger (GHZ) state

$$|\Psi'\rangle = |\tilde{0}\dots\tilde{0}\rangle + |\tilde{1}\dots\tilde{1}\rangle. \tag{3.9}$$

As seen above, an MPS need not to be normalized. In order to calculate the normalization of a translation invariant state $\langle\Psi|\Psi\rangle$, it is useful to define the transfer matrix T as

$$T = \sum_k \bar{M}^k \otimes M^k = \tag{3.10}$$

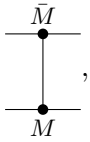

where $\bar{M^k}$ denotes the complex conjugate of M^k. The normalization of a given MPS on N sites is then $\langle\Psi|\Psi\rangle = \mathrm{Tr}(T^N)$. The transfer matrix can be furthermore understood as the matrix representation of the transfer operator $\mathbf{T}$ which admits a Kraus-representation of the form

$$\mathbf{T} : A \mapsto \sum_k (M^k)^\dagger A M^k, \tag{3.11}$$

thus it is a completely positive map. Note that the transfer matrix and transfer operator have the same spectrum. Furthermore, the transfer operator fixes the MPS tensor up to a basis choice in the physical system, due to the fact that the Kraus operators of a given completely positive map are unique up to a unitary transformation.

Note that the MPS construction does not need to be unique. In particular, any translation invariant MPS representation given by the tensor M on a finite ring can be brought into a canonical form, where $M^k = \mathrm{diag}\,(\lambda_1 L_1^k, \lambda_2 L_2^k \dots)$ is in a block-diagonal form with $0 < \lambda_j \leq 1$ and with a set of tensors $\{L_j\}_j$ which obey the following conditions for any j:

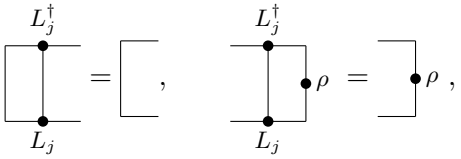

(3.12)

furthermore, $\mathbb{1}$ is the only fixed point of the transfer operators $\mathbf{T}_j$ specified by the Kraus operators L_j^k. Note that to arrive at the canonical form, blocking may be needed (cf. the example above). We will often refer to this specific canonical form as the left-canonical form, since $\mathbb{1}$ is essentially the left fixed point of the transfer operator. We say that ρ is the right fixed point of $\mathbf{T}_j$, as it is the fixed point of $\mathbf{T}_j^T$. Analogously, one can define the right-canonical form, where $\mathbb{1}$ is the right fixed point of $\mathbf{T}_j$ [19].

The translation invariant MPS defined in Eq. (3.4) is said to be an MPS with a trivial boundary. A non-trivial boundary can be given as a $D \times D$ matrix X, such that the MPS has the following form:

$$|\Psi\rangle = \sum_{k_1,\ldots k_N=0}^{d} \mathrm{Tr}\left[X M^{k_1} M^{k_2} \ldots M^{k_N}\right] |k_1 k_2 \ldots k_N\rangle =$$

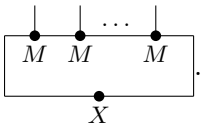

(3.13)

Let us define the map Γ_l which assigns to a $D \times D$ matrix X an MPS on l sites with a boundary X as

$$\Gamma_l :$$

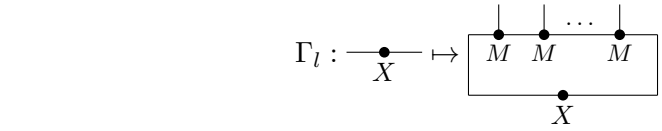

(3.14)

Now, we define injective MPS, for which several equivalent definitions have been formalized throughout the development of the MPS formalism. The most important equivalent conditions are the following:

- There exists an $l \in \mathbb{N}$ such that the map Γ_l is injective.
- The tensor M', which is the l-fold blocking of the tensor M generating the state, possesses a left inverse $(M')^{-1}$ in the sense of

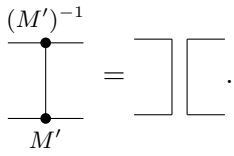

(3.15)

- The set $\{M^{k_1}, M^{k_2}, \ldots, M^{k_l} | 1 \leq k_1, \ldots, k_l \leq d\}$ spans the space of $D \times D$ matrices.

The smallest positive integer l for which the definition holds is said to be the injectivity length of the tensor M. For any natural number l' greater than the injectivity length, the tensor will automatically satisfy the conditions for injectivity.

If a translation invariant state has an injective MPS representation, its canonical form, defined by the properties in Eq. (3.12), is unique up to a unitary transformation.

We conclude this section by clarifying the nomenclature of injective MPS. The work that primarily related the MPS formalism with finitely correlated states [11] considered the injective MPS construction to be a *generic* case, while later works [20, 21] distinguished between injective and normal tensors. They restricted the definition of injectivity to tensors that have injectivity length $l = 1$. Any other tensor which has a finite injectivity length was called normal. It is clear from the definitions given above that in that nomenclature, an injective MPS is obtained by blocking l sites of a normal tensor that has injectivity length l.

3.2. C*-finitely correlated states and their relation to matrix product states

The aim of this section is first to provide the necessary mathematical prerequisites for the rest of the thesis, namely a short introduction to C*-algebras and the physically most relevant objects defined on them, following the lecture notes of Hörmann [23], and the book of Tasaki [7]. Afterwards, these necessary notions are used to define and characterize C*-finitely correlated states, which form a class of translation invariant states on an infinite spin chain. The standard introduction mainly follows the work of Fannes et al. [10, Sec. 2-4.]. While introducing the central notions of the formalism, its close relations to the MPS construction will be thoroughly highlighted, which was introduced mainly in [11]. Afterwards, we relate the pure C*-finitely correlated state construction to injective matrix product states and introduce their properties, primarily following [24].

3.2.1. Mathematical prerequisites and main definitions

A $\mathbb{C}$-vector space $\mathcal{A}$ together with an associative and bilinear multiplication map $\mathcal{A}\times\mathcal{A}\to\mathcal{A}$, $(A,B)\mapsto AB$ is called a complex algebra. A unital algebra is an algebra equipped with a unit $\mathcal{A}\ni\mathbb{1}\neq 0$. If the vector space is in addition normed, where the norm $\|.\|$ is submultiplicative, i.e. for all $A,B\in\mathcal{A}$ we have $\|AB\|\leq\|A\|\|B\|$, and $\mathcal{A}$ is complete with respect to that norm, it is called a Banach algebra. For a unital Banach algebra we require $\|\mathbb{1}\|=1$. A *-structure on $\mathcal{A}$ is a conjugate-linear map $A\mapsto A^*$ that satisfies $(AB)^*=B^*A^*$ and $(A^*)^*=A$ for each $A,B\in\mathcal{A}$. A C*-algebra $\mathcal{A}$ is a Banach-algebra together with a *-structure $A\mapsto A^*$ such that for every $A\in\mathcal{A}$, $\|A^*A\|=\|A\|^2$ holds. An element of the algebra $A\in\mathcal{A}$ is called self-adjoint if $A=A^*$. The set $\{A\in\mathcal{A}|A=BB^*\text{ for some }B\in\mathcal{A}\}$ defines the positive elements of the algebra [25].

In the conventional formalism of quantum mechanics, states are represented as density matrices, which are positive semidefinite operators on a Hilbert space with trace one. However, the notion of a quantum state can be generalized in a way, such that it constitutes a more natural way to tackle quantum systems in the thermodynamic limit. The generalization is demonstrated in the operator algebraic formalism of quantum mechanics, where the system is described by a unital C*-algebra $\mathcal{A}$. The observables of a system are the self-adjoint elements of the algebra. A quantum state in the operator algebraic formalism is a linear functional $\rho:\mathcal{A}\to\mathbb{C}$ which is positive ($\forall B\in\mathcal{A}:\rho(B^*B)\geq 0$ [25]) and preserves the unit, i.e. $\rho(\mathbb{1}_{\mathcal{A}})=1$ [7, Def. A.23]. Essentially, states are maps that take operators and assign their respective expectation values to them.

Consider a one dimensional infinite lattice, where the sites are denoted by $i\in\mathbb{Z}$, and the observables for any single site i form the C*-algebra $\mathcal{A}$, indexed by i. A finite subset Λ of the lattice can be then described with the algebra $\mathcal{A}_\Lambda$ which is characterized by placing an identical copy of $\mathcal{A}_i$ on each lattice site $i\in\Lambda$:

$$\mathcal{A}_\Lambda=\bigotimes_{i\in\Lambda}\mathcal{A}_i. \tag{3.16}$$

The extension of this notion to infinite subsets Λ of the chain is constructed by taking the C*-inductive limit of $\mathcal{A}_{\Lambda'}$ where $\Lambda' \subset \Lambda$ is a finite subset: the main idea is to identify $\mathcal{A}_{\Lambda''}$ for $\Lambda'' \subset \Lambda'$ with $\mathcal{A}_{\Lambda'}$ by an injection such that we take the tensor product of any $A \in \mathcal{A}_{\Lambda''}$ with the unit $\bigotimes_{i \in \Lambda' \setminus \Lambda''} \mathbb{1}_{\mathcal{A}_i}$. By this construction, the chain algebra $\mathcal{A}_{\mathbb{Z}}$ is also well-defined.

A translation on the chain is understood as an automorphism $\tau_p : \mathcal{A}_\Lambda \to \mathcal{A}_{\Lambda+p}$ for $p \in \mathbb{Z}$. States that are invariant under such transformations will be called translation invariant.

Let $\mathcal{A}$ be a unital C*-algebra and $\mathcal{B}$ a finite-dimensional C*-algebra, $\mathbb{E} : \mathcal{B} \otimes \mathcal{A} \to \mathcal{B}$ a completely positive map, $e \in \mathcal{B}$ positive and $\rho \in \mathcal{B}^*$ a positive functional which satisfy the following properties:

$$\mathbb{E}(e \otimes \mathbb{1}_{\mathcal{A}}) = e, \qquad \rho(\mathbb{E}(B \otimes \mathbb{1}_{\mathcal{A}})) = \rho(B) \quad \forall B \in \mathcal{B}. \tag{3.17}$$

By denoting $\mathbb{E}(B \otimes A)$ as $\mathbb{E}_A(B)$, a C*-finitely correlated state is a translation invariant state ω generated by the triple $(\mathbb{E}, \rho, e)$ such that for all $n \in \mathbb{Z}$ and $m \in \mathbb{N}$

$$\omega(A_n \otimes \cdots \otimes A_{n+m}) = \rho(e)^{-1} \rho \circ \mathbb{E}_{A_n} \circ \cdots \circ \mathbb{E}_{A_{n+m}}(e). \tag{3.18}$$

The motivation behind this construction is to characterize translation invariant states, whose correlations can be depicted by a finite dimensional object. We note that by relaxing the condition that $\mathcal{B}$ is finite-dimensional, every translation invariant state on the chain algebra could be obtained by the definition in Eq. (3.18) for a specific choice of $\mathbb{E}$ and ρ [10].

The definition for the C*-finitely correlated state is relatively broad given the freedom to choose ρ and e, but it is possible to prove that any such state can be obtained by picking $e = \mathbb{1}_{\mathcal{B}}$ to be the unit element of $\mathcal{B}$, and ρ to be a faithful state, i.e. for any $B \in \mathcal{B}$, $\rho(B^*B) = 0$ implies $B = 0$ [10, Lemma 2.5]. That particular choice slightly simplifies the expression for the expectation values of the state ω, since $\rho(\mathbb{1}_{\mathcal{B}})^{-1} = 1$.

Consider now a finite-dimensional $\mathcal{A}$. Then $\mathbb{E}$ admits a Kraus-representation, i.e. there exists some V_i such that $\mathbb{E}(B \otimes A) = \sum_i V_i^*(B \otimes A)V_i$. We now can write $\mathbb{E}$ and ρ in the graphical notation as

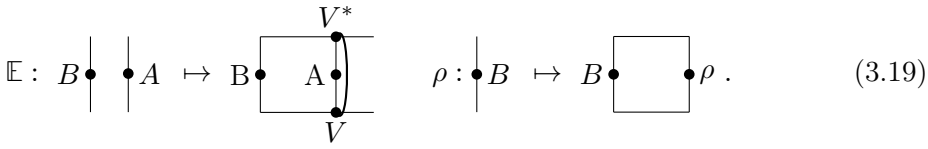

(3.19)

The "outer leg" on the first diagram corresponds to the summation over the index i. The conditions given in Eq. (3.17) can also be represented with the choice $e = \mathbb{1}_{\mathcal{B}}$ in the following way:

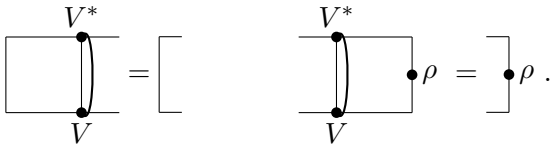

(3.20)

3.2.2. Purely generated states and ergodic decompositions

In this section we introduce the notion of purely generated C*-finitely correlated states which have the property that they can be represented on a finite-dimensional Hilbert space. We then connect the notion of such states to the MPS formalism. Furthermore, we introduce a strategy to characterize any C*-finitely correlated state by decomposing it into a convex combination of states which are extremal points in the set $\mathcal{F}$ of all C*-finitely correlated states. The statements provided in this section are proven in [10, Sec. 3-4].

A completely positive map is called pure, if it has no non-trivial decomposition into other completely positive maps. A C*-finitely correlated state on $\mathcal{A}_{\mathbb{Z}}$ that is generated by a pure $\mathbb{E}$ is called purely generated [10, Def. 4.1]. If furthermore the one-site restriction of the state ω is faithful on $\mathcal{A}$, then ω being purely generated is equivalent to that there exists some $d, D \in \mathbb{N}$ such that we can choose $\mathcal{A} = \mathcal{M}_d$ and $\mathcal{B} = \mathcal{M}_D$, and $\mathbb{E}(B \otimes A) = V^\dagger (B \otimes A) V$ holds for some $V : \mathbb{C}^D \to \mathbb{C}^D \otimes \mathbb{C}^d$ which satisfies $V^\dagger V = \mathbb{1}_{\mathbb{C}^D}$, i.e. V is a partial isometry [10, Prop. 4.2]. As a consequence, the graphical representation of $\mathbb{E}$ and its properties given initially in Eq. (3.19) and Eq. (3.20) simplifies to

$\mathbb{E}(B \otimes A) =$ 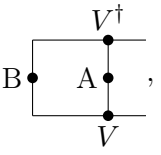

, with 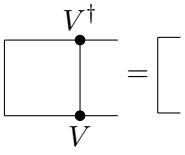

$=$
, 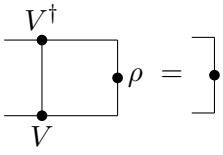

$=$ 

. (3.21)

In addition to that, if we require $\mathcal{B} = \mathcal{M}_D$, $\mathcal{A}$ to be again finite-dimensional, then to any C*-finitely correlated state ω, whose one-site restriction is faithful, we can assign a purely generated state $\tilde{\omega}$ such that there exists a faithful representation $\pi : \mathcal{A} \to \mathcal{B}(\mathcal{H})$ on the space of bounded operators on a finite-dimensional Hilbert space $\mathcal{H}$ with

$$\omega(A_n \otimes \cdots \otimes A_{n+m}) = \tilde{\omega}(\pi(A_n) \otimes \cdots \otimes \pi(A_{n+m})). \tag{3.22}$$

Furthermore, $\tilde{\omega}$ is generated by the pure map $\tilde{\mathbb{E}} : \mathcal{M}_D \otimes \mathcal{B}(\mathcal{H}) \to \mathcal{M}_D$ such that for any $B \in \mathcal{M}_D$, $\tilde{\mathbb{E}}(B \otimes \mathbb{1}_{\mathcal{B}(\mathcal{H})}) = \mathbb{E}(B \otimes \mathbb{1}_{\mathcal{A}})$ [10, Prop. 4.2]. Note that $\tilde{\omega}$ is a state on the chain $\mathcal{B}(\mathcal{H})_{\mathbb{Z}}$ and will be called the dilation of ω.

We now restrict ourselves to purely generated C*-finitely correlated states and show that any such state has a translation invariant MPS representation. Let $\mathcal{A} = \mathcal{M}_d$, $\mathcal{B} = \mathcal{M}_D$ which are represented on the finite-dimensional Hilbert spaces $\mathbb{C}^d$ and $\mathbb{C}^D$, respectively. Let $\hat{\mathbb{E}}(B) \coloneqq \mathbb{E}_{\mathbb{1}_{\mathcal{M}_d}}(B) = \mathbb{E}(B \otimes \mathbb{1}_{\mathcal{M}_d})$ be pure, i.e. $\hat{\mathbb{E}}(B) = V^\dagger (B \otimes \mathbb{1}_{\mathcal{M}_d}) V$. We set

$$V = \sum_{\alpha,\beta,k} M^k_{\alpha\beta} |\alpha k\rangle\langle\beta|, \tag{3.23}$$

which then implies that $\hat{\mathbb{E}}(B) = \sum_k (M^k)^\dagger B M^k$. This is exactly the Kraus representation (i.e. Eq. (3.11)) of the transfer operator $\mathbf{T}$ generated by the MPS tensor M defined in Eq. (3.1). The distinction between V and M is only an instance of reshaping: V is

regarded to be a vector in the space $\mathbb{C}^D \otimes \mathbb{C}^d \otimes (\mathbb{C}^D)^*$, while $M \in \mathbb{C}^D \otimes (\mathbb{C}^D)^* \otimes \mathbb{C}^d$. The conditions given in Eq. (3.21) correspond to the properties of the canonical form of the MPS representation defined in Eq. (3.12).

The object $\hat{\mathbb{E}}$ also serves as an important tool to calculate correlation functions and to characterize a set of states that turns out to be extremely useful for describing any C*-finitely correlated state. The first condition in Eq. (3.17) ensures that $\mathbb{1}_{\mathcal{B}}$ is an eigenvector of $\hat{\mathbb{E}}$ with eigenvalue one, but does not exclude degeneracies in general. If we require $\hat{\mathbb{E}}$ to be irreducible, i.e. there exists no non-trivial projector P that satisfies $\hat{\mathbb{E}}(B) = P\hat{\mathbb{E}}(B)P^\dagger$ for all $B = PBP^\dagger$, then $\mathbb{1}_{\mathcal{B}}$ is the only eigenvector of $\hat{\mathbb{E}}$ with eigenvalue one [21]. The states generated by such $\mathbb{E}$ are then called ergodic, and they are extremal points in the convex set of all translation invariant states $\mathcal{T}$. To characterize ergodic C*-finitely correlated states we need less independent data, since then the adjoint of $\hat{\mathbb{E}}$ is also irreducible, so ρ is uniquely determined by $\hat{\mathbb{E}}$ up to a scalar. Furthermore, any C*-finitely correlated state can be written as a unique convex combination of ergodic C*-finitely correlated states, by constructing the algebra $\mathcal{B}$ as a direct sum of algebras of the form $\mathcal{B}_P = P\mathcal{B}P^\dagger$, where P is any non-trivial minimal projector projecting onto the 1-eigenspace of $\mathbb{E}_{\mathbb{1}_{\mathcal{A}}}$. By restricting $\mathbb{E}_A$ and ρ to any such algebra, the state generated by the restrictions is an ergodic C*-finitely correlated state [26].

If we consider the case where the state is purely generated, then it has an MPS representation in the canonical form. The decomposition into ergodic states corresponds to the block-diagonal form of the MPS, where each block represents an ergodic C*-finitely correlated state, whose transfer operator has 1 as a unique eigenvalue. Note that the ergodic decomposition is unique, but it does not imply the uniqueness of the canonical form, since the MPS representation of each ergodic state is not necessarily unique. Furthermore, one can always assume without loss of generality that the largest eigenvalue of the transfer matrix is one.

The definition of ergodicity does not exclude eigenvalues of $\hat{\mathbb{E}}$ that are of the form $e^{i\vartheta}$ for some $\vartheta \in (0, 2\pi)$. The set of eigenvalues of $\hat{\mathbb{E}}$ with absolute value one will be called the peripheral spectrum of $\hat{\mathbb{E}}$. For an ergodic C*-finitely correlated state generated by $(\mathbb{E}, \rho, \mathbb{1}_{\mathcal{B}})$, there exists $p \in \mathbb{N}$ such that the peripheral spectrum of $\hat{\mathbb{E}}$ is the set $\{\exp(2\pi i n/p) \,|\, n = 0, \ldots, p-1\}$. The eigenvectors corresponding to these eigenvalues are unique and can be chosen as unitary matrices in $\mathcal{B}$. Furthermore, any ergodic C*-finitely correlated state can be written uniquely as the superposition of p p-periodic C*-finitely correlated states (namely states, which are C*-finitely correlated on the chain $(\mathcal{A}^{\otimes p})_{\mathbb{Z}}$) that are translates of each other [10, Prop. 3.3]. As a consequence, any C*-finitely correlated state can be uniquely decomposed as a finite convex combination of periodic C*-finitely correlated states, that are extremal points of $\mathcal{F}$.

For C*-finitely correlated states, that have no further decomposition into periodic states, the peripheral spectrum of $\hat{\mathbb{E}}$ is trivial, so $\hat{\mathbb{E}}^n(B)$ converges exponentially fast to $\rho(B) \cdot \mathbb{1}_{\mathcal{B}}$ for any $B \in \mathcal{B}$. Since the correlation functions of these states have the form

$$\omega(A_n \otimes \mathbb{1}_{\mathcal{A}} \otimes \cdots \otimes \mathbb{1}_{\mathcal{A}} \otimes A_{n+m}) = \rho \circ \mathbb{E}_{A_n} \circ \hat{\mathbb{E}}^{m-n-1} \circ \mathbb{E}_{A_{n+m}}(\mathbb{1}_{\mathcal{B}}), \tag{3.24}$$

this special class of states exhibits an exponential decay of correlations, thus these states will be called exponentially clustering.

The possibility of such decompositions is now illustrated with a simple example. The equal weight superposition of Néel-ordered spin-1/2 states introduced in Eq. (3.6) possesses an MPS representation (see Eq. (3.7)), thus it is a purely generated C*-finitely correlated state in the thermodynamic limit. The spectrum of its transfer matrix is $\{1, -1, 0, 0\}$, so it is ergodic and has to be a superposition of two states, that are 2-periodic, one-site translations of each other and finitely correlated on the chain $((\mathcal{M}^d)^{\otimes 2})_{\mathbb{Z}}$. The first two properties are straightforward from the definition of the state, and after blocking (cf. Eq. (3.8) and Eq. (3.9)) the periodic components correspond to $|\tilde{0}\dots\tilde{0}\rangle$ and $|\tilde{1}\dots\tilde{1}\rangle$, respectively. Note that these states individually are product states on $((\mathcal{M}^d)^{\otimes 2})_{\mathbb{Z}}$, their MPS representations are injective.

To summarize, any C*-finitely correlated state ω can be studied by first taking its dilation $\tilde{\omega}$ defined in Eq. (3.22), which is purely generated and can be represented on a finite-dimensional Hilbert space, so $\tilde{\omega}$ admits an MPS representation in the left canonical form. Since we required $\tilde{\mathbb{E}}(B \otimes \mathbb{1}_{\mathcal{B}(\mathcal{H})}) = \mathbb{E}(B \otimes \mathbb{1}_{\mathcal{A}})$, the ergodic properties of the dilation are the same as of the original state ω. As a consequence, each block in the block-diagonal canonical form corresponds to an ergodic state, which is then a superposition of periodic, exponentially clustering states. The number of such states in the superposition depends on the peripheral spectrum of the transfer matrix. Hence, the basic building blocks of any C*-finitely correlated state are the translation invariant matrix product states, whose transfer matrix has only one eigenvalue with absolute value one. Now, we will discuss the most important properties of these states.

3.2.3. Properties of injective MPS

In this section we connect the notion of pure C*-finitely correlated states with the injective MPS construction. Furthermore, we introduce the notion of parent Hamiltonians, which can be constructed from an injective MPS, and has it as a unique ground state. We conclude this section by further remarks regarding the parent Hamiltonians of block-injective MPS.

Due to the fact that the transfer matrix of a pure C*-finitely correlated state has a trivial peripheral spectrum, for a large enough system size N we can approximate its N-th power by:

$T^N \approx$ 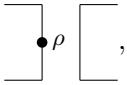 , (3.25)

as the following inequality holds [10, Lemma 5.2]:

$$a(N) \coloneqq \mathrm{Tr}(\rho^{-1})\|T^N - T^\infty\| \leq D^2\lambda^N, \tag{3.26}$$

where λ is the absolute value of the second largest eigenvalue of T.

We can now define the map $\Gamma_l : \mathcal{M}^D \to (\mathbb{C}^d)^{\otimes l}, X \mapsto \sum_{k_1,\ldots,k_l} \mathrm{Tr}(XM^{k_1}\ldots M^{k_l})|k_1\ldots k_l\rangle$ analogously to Eq. (3.14) introduced in the MPS formalism. Now, $\mathcal{B} = \mathcal{M}_D$ is considered to be a Hilbert space with inner product specified by ρ: for $X, Y \in \mathcal{B}$ we have $\langle X, Y\rangle_\rho = \mathrm{Tr}(\rho X^\dagger Y)$. Furthermore, the norm of $X \in \mathcal{B}$ induced by that inner product is denoted by $\|X\|_\rho$. The standard inner product and norm on any $\mathbb{C}^d$ are labeled without ρ. From the inequality [10, Lemma 5.2]

$$|\langle \Gamma_l(X), \Gamma_l(Y)\rangle - \langle X, Y\rangle_\rho| \leq a(l)\|X\|_\rho\|Y\|_\rho \tag{3.27}$$

it follows that the maps Γ_l are injective for a large enough l [10], and the fact that the quantity

$$a_-(l) = \inf_{X\neq 0} \frac{\|\Gamma_l(X)\|^2}{\|X\|_\rho^2} \geq 1 - a(l), \tag{3.28}$$

which vanishes if and only if Γ_l is not injective, is monotonously increasing in l shows that for any $l' \geq l$, $\Gamma_{l'}$ is injective if Γ_l is injective [10, Lemma 5.3]. As a consequence, we can represent exponentially clustering (i.e. states that exhibit an exponential decay of correlations) purely generated C*-finitely correlated states with injective matrix product states. The smallest natural number l for which Γ_l is injective is then the injectivity length of the MPS. Furthermore, since these states cannot be written even as a superposition of non-periodic states, in the finitely correlated state formalism they are also called pure [27].

Parent Hamiltonians

We now show, that for any injective MPS on a finite ring we can construct a Hamiltonian which has a unique ground state in the form of the given injective MPS [24, Thm. 3.5]. We refer to such Hamiltonians as the parent Hamiltonian of the MPS.

Let $|\Psi\rangle$ be a state generated by an injective tensor M with injectivity length l. We denote the range of the map Γ_l by $\mathcal{G}_l$ and the orthogonal projector onto that space by G_l. Let us define the Hermitian projector acting non-trivially on $l+1$ sites by

$$h_i = \mathbb{1}_d^{\otimes(i-1)} \otimes (\mathbb{1}_d^{\otimes(l+1)} - G_{l+1}) \otimes \mathbb{1}_d^{\otimes(N-l-i)}, \tag{3.29}$$

with $\mathbb{1}_d \coloneqq \mathbb{1}_{\mathcal{M}_d}$. By construction, h_i is a positive semidefinite local Hamiltonian, thus its lowest possible eigenvalue is zero. Furthermore, $|\Psi\rangle$ is a zero-energy state of h_i. We extend the Hamiltonian to the whole N-body ring as

$$H = \sum_{i=1}^{N} h_i. \tag{3.30}$$

The sites are defined to be modulo N, i.e. $N + l \coloneqq l$ due to periodic boundary conditions. In order to prove that $|\Psi\rangle$ is the unique ground state of H, we need some additional

properties of injective matrix product states.

Let M and N be injective tensors with injectivity length 1. Then they satisfy the intersection property [24, Thm. 3.3]

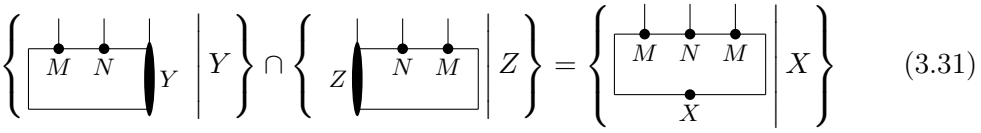

(3.31)

where Y, Z are tensors consisting of $D \times D$ matrices for each physical degree of freedom, and $X \in \mathcal{M}_D$. If we set N to be the $(k-1)$-fold blocking of M, meaning that in Eq. (3.31) each index for N corresponds to $(k-1)$ sites as given generally in Eq. (3.5), then an immediate consequence of the intersection property is that $(\mathcal{G}_k \otimes \mathbb{C}^d) \cap (\mathbb{C}^d \otimes \mathcal{G}_k) = \mathcal{G}_{k+1}$. By induction, this result can be extended to any chain with system size N:

$$\mathcal{G}_N = \bigcap_{i=0}^{N-2} (\mathbb{C}^d)^{\otimes i} \otimes \mathcal{G}_2 \otimes (\mathbb{C}^d)^{\otimes(N-2-i)}, \tag{3.32}$$

and to any tensor with injectivity length l for any $N \geq l' > l$ as

$$\mathcal{G}_N = \bigcap_{i=0}^{N-l'} (\mathbb{C}^d)^{\otimes i} \otimes \mathcal{G}_{l'} \otimes (\mathbb{C}^d)^{\otimes(N-l'-i)}. \tag{3.33}$$

The intersection property implies explicitly, that the intersection of l'-body supports is exactly the ground space of the N-body chain. The following relevant property for the proof is the closure property [24, Thm. 3.4]

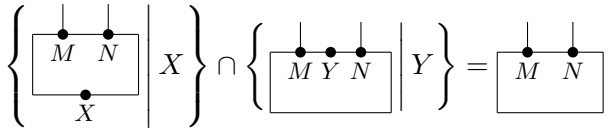

(3.34)

for MPS M and N with injectivity length $l = 1$. The generalization to MPS with larger injectivity length follows straightforwardly by l-fold blocking, since the proof in [24] only requires the tensors M and N to possess a left inverse. We now decompose the Hamiltonian as $H = H_L + H_R$ with $H_L = h_1 + \frac{1}{2}h_2 + \cdots + \frac{1}{2}h_{N-1}$ and $H_R = \frac{1}{2}h_2 + \frac{1}{2}h_3 + \cdots + \frac{1}{2}h_{N-1} + h_N$. The intersection of the kernels of H_L and H_R is exactly the space $\mathcal{G}_l$ by the closure property. Due to the positive semidefiniteness of the Hamiltonian we conclude that $|\Psi\rangle$ is the unique ground state of the Hamiltonian in Eq. (3.30) defined by the sum of local terms in Eq. (3.29). These results hold for infinite translation invariant systems as well, but there it is more useful to switch back to the pure C*-finitely correlated state formalism, the exact proofs are found in [10, Sec. 5].

The fact that the injective MPS is the unique ground state of its parent Hamiltonian holds only for periodic boundary conditions, when a finite system size is considered.

For open boundaries, we have an extra degree of freedom just from the construction of $\mathcal{G}_N$, thus the open chain parent Hamiltonian is going to exhibit a D^2-fold ground state degeneracy. However, by taking the thermodynamic limit (note, that the state is then only well-defined as a linear functional) the state will not depend on the choice of the boundary [7, Sec. 7.2.3]. As a consequence, an injective MPS is the unique ground state of its parent Hamiltonian in the thermodynamic limit, independent of the boundary.

We now provide a generalization of the intersection property that was proven in [28, Prop. 7]. First, we need a definition of the overlap $\mathcal{O}$ between two subspaces $\mathcal{H}_1$ and $\mathcal{H}_2$ of a larger Hilbert space $\mathcal{H}$:

$$\mathcal{O}(\mathcal{H}_1, \mathcal{H}_2) := \sup_{\substack{|\phi_1\rangle \in \mathcal{H}_1 \setminus \{0\} \\ |\phi_2\rangle \in \mathcal{H}_2 \setminus \{0\}}} \frac{|\langle \phi_1 | \phi_2 \rangle|}{\||\phi_1\rangle\| \cdot \||\phi_2\rangle\|} \tag{3.35}$$

A translation invariant state, which is a convex combination of distinct matrix product states generated by the tensors $\{M^{(1)}, \ldots, M^{(n)}\}$, satisfies the property in Eq. (3.33) for $l' \geq m$ if the following hold:

- Each tensor $M^{(i)}$ satisfies the property given in Eq. (3.33) for m sites.
- The overlap of any $\mathcal{G}_m^{(i)}$ and $\mathcal{G}_m^{(j)}$ is strictly smaller than $1/(n-1)$ for $i \neq j$, where $\mathcal{G}_m^{(i)}$ denotes the range of $\Gamma_m^{(i)} : X \mapsto \sum_{k_1, \ldots k_m} \mathrm{Tr}(X M^{(i),k_1} \ldots M^{(i),k_m}) |k_1 \ldots k_m\rangle$.

Especially, if an MPS is block-injective (i.e. each block in the canonical form corresponds to an injective MPS), and each block generates a distinct state, one can easily check the validity of that property for a large enough m by calculating the overlaps of each subspace generated by the injective blocks. Note that m is always larger than the injectivity length of any individual block.

For a block-injective MPS, one can construct a parent Hamiltonian in a similar fashion by taking a projection onto the orthogonal complement of $\bigoplus_i \mathcal{G}_m^{(i)}$ for a sufficiently large m [11]. However, the number of blocks in the canonical form, which generate a distinct state, corresponds to the ground state degeneracy of the parent Hamiltonian, so any convex combination of the injective matrix product states that generate the state is going to be a zero-energy state of the parent Hamiltonian [28, Thm. 1].

4. The ground state gap

This chapter aims to introduce two methods to prove the existence and to bound the spectral gap of a translation invariant frustration-free local Hamiltonian.

Firstly, Knabe's method [9] is described, which provides a lower bound on the spectral gap by utilizing finite-size criteria. Originally, the method was constructed for Hamiltonians that have periodic boundary conditions, but the argument was also extended to systems with open boundaries [18].

Then, versions of the martingale method [28], which are tailored for one-dimensional systems, are also discussed. These strategies serve as a proof for the existence of the gap, given that certain criteria are fulfilled regarding the structure of the Hamiltonian and its respective ground states. The method also provides an explicit expression for the lower bound of the gap, which takes a particularly useful form if the ground states are all injective matrix product states, and there are only a finite amount of them in the thermodynamic limit. By utilizing the tensor network notation presented in one of the previous chapters, a simplified proof is provided for the case when the Hamiltonian has a unique injective MPS as its ground state. The original proof is based on [10, Lemma 6.2], whose result takes a relatively simple form for parent Hamiltonians of injective MPS. If the ground state is degenerate, similar arguments were utilized in [28] and [29] to arrive at an explicit bound, which then depends also on the overlap of the respective ground spaces. However, the proofs provided there would not become simpler by the use of tensor network notation, thus only the key ideas are discussed to arrive at the bound. Furthermore, a corrected estimate depending on the maximum overlap between any ground spaces is provided, which yields a less strict bound than in [28, Prop. 12].

It is worthwhile to mention that the standard martingale method for quantum spin systems is more general than what the discussion in this thesis covers, since it was constructed for lattices of any dimension and arrangement, whereas we only focus now on spin chains.

4.1. Knabe's method

In Knabe's 1988 work [9], a lower bound on the ground state gap of a special class of many-body Hamiltonians was derived. Let $P_{i,i+1}$ be a projector on a spin chain that acts on two spins on neighboring sites i and $i+1$. The Hamiltonian H on an N-site ring (i.e. periodic boundary conditions are considered) is of the form

$$H = \sum_{i=1}^{N} P_{i,i+1}. \tag{4.1}$$

In addition, it is assumed that the ground state energy of the system is zero. Then H having an energy gap which is at least ϵ is equivalent to the inequality

$$H^2 - \epsilon H \geq 0. \tag{4.2}$$

In order to derive a condition for the existence of a gap, a smaller subsystem with open boundaries is considered on $(n+1) < N$ sites, starting from site i. Assume that the energy gap ϵ_n of the subsystem Hamiltonian $h_{n,i}$ given by

$$h_{n,i} = \sum_{j=i}^{i+n-1} P_{j,j+1}, \quad \text{with} \quad (h_{n,i})^2 - \epsilon_n h_{n,i} \geq 0 \tag{4.3}$$

is known. The aim now is to relate the gap of the subsystem Hamiltonian to the gap of the global Hamiltonian H. Firstly, we take the square of the subsystem Hamiltonian

$$(h_{n,i})^2 = h_{n,i} + \sum_{j=i}^{i+n-2} (P_{j,j+1}P_{j+1,j+2} + P_{j+1,j+2}P_{j,j+1}) + \sum_{k=2}^{i+n-2} \sum_{j=i}^{i+n-k-1} 2P_{j,j+1}P_{j+k,j+k+1}, \tag{4.4}$$

where we utilized $P_{i,i+1}^2 = P_{i,i+1}$ and $[P_{j,j+1}, P_{j+k,j+k+1}] = 0$ for $(k-j) > 1$. Now we sum each term for all $i = 1, \ldots, N$ and exploit the fact that the system is defined on a ring, so each site is defined modulo N. We can thus write

$$\sum_{i=1}^{N} h_{n,i} = \sum_{i=1}^{N} \sum_{j=i}^{i+n-1} P_{j,j+1} = \sum_{i=1}^{N} (P_{i,i+1} + P_{i+1,i+2} + \cdots + P_{i+n-1,i+n}) = n \cdot H, \tag{4.5a}$$

$$\sum_{i=1}^{N} \sum_{j=i}^{i+n-2} (P_{j,j+1}P_{j+1,j+2} + P_{j+1,j+2}P_{j,j+1}) = (n-1) \sum_{j=1}^{N} (P_{j,j+1}P_{j+1,j+2} + P_{j+1,j+2}P_{j,j+1}), \tag{4.5b}$$

$$\sum_{i=1}^{N} \sum_{k=2}^{i+n-2} \sum_{j=i}^{i+n-k-1} 2P_{j,j+1}P_{j+k,j+k+1} = \sum_{k=2}^{n-1} (n-k) \sum_{j=1}^{N} 2P_{j,j+1}P_{j+k,j+k+1}. \tag{4.5c}$$

Now, it is going to be useful to divide by $(n-1)$:

$$\frac{\sum_{i=1}^{N}(h_{n,i})^2}{n-1} = \frac{n\cdot H}{n-1} + \sum_{j=1}^{N}(P_{j,j+1}P_{j+1,j+2} + P_{j+1,j+2}P_{j,j+1}) + \sum_{k=2}^{n-1}\frac{n-k}{n-1}\sum_{j=1}^{N} 2P_{j,j+1}P_{j+k,j+k+1}. \tag{4.6}$$

The sum over the anticommutator of the overlapping projectors does not need to be positive semidefinite. However, all the other terms in the expression are certainly positive semidefinite. By expanding H^2 as

$$H^2 = H + \sum_{j=1}^{N}(P_{j,j+1}P_{j+1,j+2} + P_{j+1,j+2}P_{j,j+1}) + \sum_{k=2}^{n-1}\sum_{j=1}^{N} 2P_{j,j+1}P_{j+k,j+k+1}, \tag{4.7}$$

the same sum is obtained over the anticommutator of overlapping projectors, but the summands of the last sum appear with a larger prefactor, it follows that

$$\frac{\sum_{i=1}^{N}(h_{n,i})^2}{n-1} \leq \frac{1}{n-1}H + H^2. \tag{4.8}$$

By utilizing the gap inequality of the subsystem Hamiltonian given in Eq. (4.3) we arrive at an inequality that relates the energy gap ϵ of the global Hamiltonian to the gap ϵ_n of the subsystem Hamiltonian

$$H^2 \geq \frac{1}{n-1}\left(\sum_{i=1}^{N}(h_{n,i})^2 - H\right) \geq \frac{n}{n-1}\left(\epsilon_n - \frac{1}{n}\right)H \Rightarrow \epsilon \geq \frac{n}{n-1}\left(\epsilon_n - \frac{1}{n}\right). \tag{4.9}$$

As a consequence, a finite-size gap ϵ_n that is larger than $1/n$ implies an energy gap on H that is independent of the system size N. Thus, this method becomes extremely useful for calculating energy gaps in the thermodynamic limit.

In [18], Hamiltonians of the same form were considered but on an open chain, so they cannot be written as a sum given in Eq. (4.5a), but rather as the extension of the smaller, open Hamiltonian in Eq. (4.3) to the whole chain. In addition, we can decompose it into two sums with $k < n$:

$$H = \sum_{i=1}^{N-1} P_{i,i+1} = h_{N-1,1} = \sum_{i=1}^{N-1} h_{1,i} = \frac{1}{n}\left[\sum_{i=1}^{N-n} h_{n,i} + \sum_{k=1}^{n-1}(h_{k,1} + h_{k,N-k})\right]. \tag{4.10}$$

The square of the Hamiltonian can be expanded as in Eq. (4.4) with system size N as:

$$H^2 = H + \sum_{j=1}^{N-2}(h_{1,j}h_{1,j+1} + h_{1,j+1}h_{1,j}) + \sum_{k=2}^{N-2}\sum_{j=1}^{N-k-1}(h_{1,j}h_{1,j+k} + h_{1,j+k}h_{1,j}). \tag{4.11}$$

Furthermore, it is possible to rearrange the terms to arrive at the form

$$H^2 = H + \sum_{k=1}^{n-1} \sum_{j=1}^{N-k-1} (h_{1,j}h_{1,j+k} + h_{1,j+k}h_{1,j}) + \sum_{|i-j|>n-1} h_{1,i}h_{1,j}, \tag{4.12}$$

where an inequality is obtained by discarding the positive semidefinite terms from the last sum and include the positive semidefinite expressions from the first sum with less weight:

$$H^2 \geq H + \sum_{k=1}^{n-1} \frac{n-k}{n-1} \sum_{j=1}^{N-k-1} (h_{1,j}h_{1,j+k} + h_{1,j+k}h_{1,j}). \tag{4.13}$$

Here, less weight means that by writing out the projectors explicitly, it is straightforward to see that each term of the form $P_{j,j+1}P_{j+k,j+k+1}$ appears in the sum $(n-k)/(n-1)$ times. As a consequence, terms which are not necessarily positive semidefinite will still appear exactly as in the square of the total Hamiltonian. Now, we rewrite the expression above such that it becomes possible to include the local gap, while the weights of the projector terms remains the same:

$$H^2 \geq H + \frac{1}{n-1} \left(\sum_{j=1}^{N-n} h_{n,j}^2 + \sum_{k=1}^{n-1} (h_{k,1}^2 + h_{k,N-k}^2) - n \cdot H \right). \tag{4.14}$$

Then, by using the local gap and the decomposition in Eq. (4.10), we obtain a result similar to the periodic case, the only difference is the fact that a minimum of all local gaps up to system size $n+1$ is present in the expression:

$$H^2 \geq H + \frac{1}{n-1} \left(\min_{k=1,\ldots,n} \epsilon_k - n \right) H = \frac{n}{n-1} \left(\min_{k=1,\ldots,n} \epsilon_k - \frac{1}{n} \right) H. \tag{4.15}$$

Note that all Hamiltonians considered in the setup are frustration-free. For nearest-neighbor frustration-free Hamiltonians that are not sums of projectors, the Knabe bound is still a useful estimate. Consider such a Hamiltonian on a d-level spin system with ground state degeneracy $p < d^2$ and zero ground state energy. By calculating the spectral decomposition of any local term $\tilde{H}_{i,i+1}$ we arrive at the bound

$$\tilde{H}_{i,i+1} \geq \tilde{\epsilon}_2 \cdot P_{i,i+1}, \tag{4.16}$$

where $\tilde{\epsilon}_2$ is the second smallest eigenvalue of $\tilde{H}_{i,i+1}$, and $P_{i,i+1}$ is the projector onto the orthogonal complement of the ground space. This relation implies that the gap of $\tilde{H} = \sum_i \tilde{H}_{i,i+1}$ is bounded from below by $\tilde{\epsilon}_2 \cdot \epsilon$.

4.2. The martingale method

4.2.1. General strategies for spin chains

Before providing the general method for frustration-free spin chain models, we start with a simple case, where we only rely on nearest-neighbor Hamiltonians on a finite open chain. This method provides a bound on the spectral gap, but it is possible to extend the argument to prove the existence of the spectral gap of a wider range of models. The general idea of the extension is to rely on local Hamiltonians with a larger interaction range. This alone broadens the applicability of the method, in later chapters it will also turn out to be more powerful for nearest-neighbor parameterized local interactions. For two-body interactions, a local Hamiltonian with a larger interaction range is built by adding up the nearest-neighbor terms, and then by summing up each translation of the local term to extend it to the whole chain. After providing a gap for those Hamiltonians, it is straightforward to rescale the bound with the prefactor of the two-body term which appears the most in the larger-range Hamiltonian. The generality of this method is based on the fact that for Hamiltonians with a larger interaction range we can provide a bound on the overlaps of the ground spaces on more sites. We also introduce a slightly different strategy, where we start from a translation invariant Hamiltonian with a finite interaction range, from which we then construct a two-body interaction with the same ground space on a regrouped spin chain. This allows for the bound on the ground space overlaps on an arbitrary number of sites, while leaving the rescaling parameter independent of the interaction range.

We first consider a Hamiltonian H_N on an open N-body chain which is the sum of identical two-body terms

$$H_N = \sum_{i=1}^{N-1} h_{i,i+1}. \tag{4.17}$$

The Hamiltonian is assumed to be frustration-free and to have zero ground state energy. In addition, we assume that the two-body Hamiltonian $h_{i,i+1}$ possesses a spectral gap ϵ_2, and thus

$$h_{i,i+1} \geq \epsilon_2(\mathbb{1} - G_{i,i+1}), \tag{4.18}$$

where $G_{i,i+1}$ is the orthogonal projection onto the two-body ground state space on the sites i and $i+1$. The martingale method ensures that the existence of the spectral gap is related to the overlap of certain ground space projectors. Define the quantity

$$E_i = \begin{cases} \mathbb{1} - G_{1,2} & i = 1 \\ G_{1,\ldots,i} - G_{1,\ldots,i+1} & i \in \{2, \ldots, N-1\} \\ G_{1,\ldots,N} & i = N \end{cases}, \tag{4.19}$$

where $G_{1,\ldots,i}$ denotes the orthogonal projection onto the ground space on the sites 1 to $i > 1$. Due to the fact that the ground space projections commute if their domains are either disjoint or one is entirely contained in the other, the set $\{E_i\}_{i=1}^N$ consists of mutually orthogonal projections that sum up to the identity, i.e. we have

$$E_n E_m = \delta_{n,m} E_n, \qquad E_n^\dagger = E_n, \qquad \sum_{i=1}^{N} E_i = \mathbb{1}. \tag{4.20}$$

The martingale method provides a lower bound on the ground state gap if

$$\|G_{i,i+1} E_i\| = \|G_{1,\ldots,i} G_{i,i+1} - G_{1,\ldots,i+1}\| \leq \gamma < \frac{1}{\sqrt{2}} \qquad \forall i \in \{1, \ldots, N-1\}. \tag{4.21}$$

If this condition on the overlaps of the ground state projections is satisfied along with the frustration-free condition given in Eq. (4.18), then the Hamiltonian given in Eq. (4.17) has a ground state gap ϵ, which satisfies the bound [28, Thm. 3]

$$\epsilon \geq \epsilon_2 (1 - \sqrt{2} \cdot \gamma)^2. \tag{4.22}$$

A γ smaller than $1/\sqrt{2}$ independent of the system size implies that the Hamiltonian has a spectral gap in the thermodynamic limit.

The martingale method thus provides a powerful argument to prove the existence of the ground state gap in the thermodynamic limit without relying on a finite-size gap: for frustration-free translation invariant local Hamiltonians the only relevant condition for the existence of the gap is Eq. (4.21), which does not depend on the gap of any subsystem Hamiltonian, but rather on the overlap of ground space projections from which γ can be calculated. However, the overlap on a single site (in Eq. (4.21) it is the site labeled by i) does not generally satisfy the condition given in Eq. (4.21) for gapped Hamiltonians and thus does not detect the gap. To extend the argument provided beforehand, we consider a Hamiltonian $\tilde{H}$, which is assumed to be bounded from both sides by H times a constant:

$$c \cdot H \leq \tilde{H} \leq C \cdot H. \tag{4.23}$$

This strategy allows for the calculation of overlaps of ground space projectors on a larger region than a single site, since we can add up the two-body local Hamiltonians to construct a new local Hamiltonian with a larger interaction range. Since a single nearest neighbor term can appear more than once in the global Hamiltonian, the new Hamiltonian $\tilde{H}$ should be bounded by a constant times the original Hamiltonian H. For spin chain systems with nearest neighbor interactions, a natural choice of $\tilde{H}$ could be to pick a finite length $l < N/2$ and consider $(l+1)$-site local terms

$$\tilde{h}_{i,i+l} = \sum_{j=i}^{l-1} h_{i,i+1}, \tag{4.24}$$

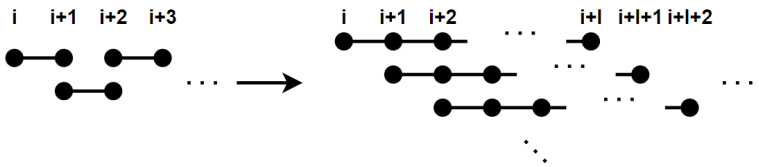

Figure 4.1.: Schematic representation of Eq. (4.24) and Eq. (4.25)

and a Hamiltonian which arises as the sum of all translations of the local terms:

$$\tilde{H} = \sum_{i=1}^{N-l} \tilde{h}_{i,i+l}. \tag{4.25}$$

The construction of $\tilde{h}_{i,i+l}$ and $\tilde{H}$ is represented in Fig. 4.1 with the nodes representing the spins and the lines between the nodes corresponding to the interactions. Each term $h_{i,i+1}$ appears in $\tilde{H}$ at most l times, so for our case the choices $c = 1$ and $C = l$ in Eq. (4.23) are justified. Now, it is possible to extend the conditions Eq. (4.18) and Eq. (4.21) for a Hamiltonian which is of the form as in Eq. (4.23) by calculating the $(l+1)$-site local gaps

$$\tilde{h}_{i,i+l} \geq \epsilon_{l+1}(\mathbb{1} - G_{i,\ldots,i+l}) \tag{4.26}$$

and by bounding the l-site overlaps of ground space projections

$$\|G_{1,\ldots,i}G_{i-l+1,\ldots,i+1} - G_{1,\ldots,i+1}\| \leq \gamma_l < \frac{1}{\sqrt{l+1}} \qquad \forall i \in \{l, \ldots, N-1\}, \tag{4.27}$$

we arrive at a more general expression for the gap, if the conditions in Eq. (4.26) and Eq. (4.27) are satisfied for one and the same l [28, Thm. 3]:

$$\epsilon \geq \frac{\epsilon_{l+1}}{l}(1 - \sqrt{l+1} \cdot \gamma_l)^2. \tag{4.28}$$

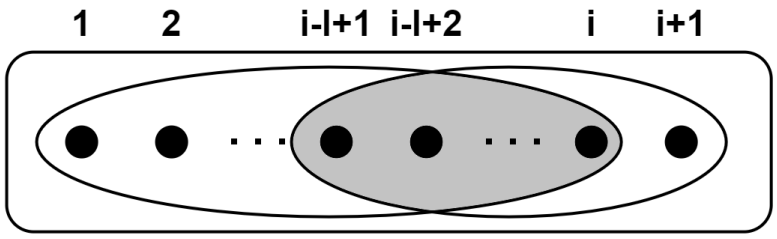

Figure 4.2.: Schematic representation of the left-hand side of Eq. (4.27)

A schematic representation of the left-hand side of Eq. (4.27) is shown in Fig. 4.2, where the gray area corresponds to the overlapping region on l sites. It is clear that the bound obtained in Eq. (4.28) is applicable for translation invariant Hamiltonians that are not necessarily composed only of nearest neighbor interactions, but rather have an interaction range of at most $l+1$. We also see that Eq. (4.22) is the special case of Eq. (4.28) for $l=1$. Again, the proof of the existence of the gap reduces to the calculation of γ_l for a large enough l, and we only require local gaps if we want to obtain an explicit bound on the gap.

For models with interaction range at most $l+1$, it is possible to obtain a result, where the bound for the gap does not have an explicit l-dependency. The strategy is to bound the finite-range Hamiltonian by a nearest-neighbor Hamiltonian with the same ground space on a regrouped chain, such that the number of reappearing local terms remains bounded. Consider a translation invariant frustration-free Hamiltonian H of the form

$$H = \sum_{i=1}^{N-l} h_{i,\ldots,i+l}, \tag{4.29}$$

and take an integer $p > l$ such that $N/p := m \in \mathbb{N}$. Let us construct the nearest neighbor terms of the Hamiltonian $\tilde{H} = \sum_{i'=1}^{m-2} \tilde{h}_{i',(i+1)'}$ on the regrouped chain as

$$\tilde{h}_{i',(i+1)'} = \sum_{j=1}^{2p-l} h_{pi'+j,\ldots,pi'+j+l}. \tag{4.30}$$

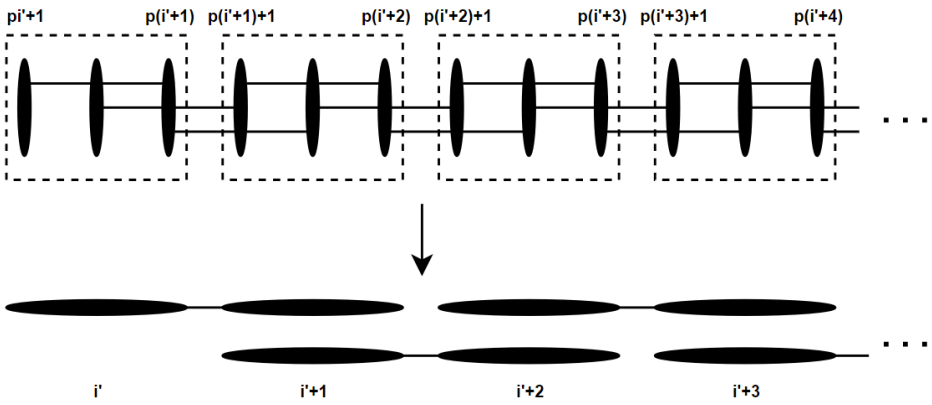

Figure 4.3.: Schematic representation of the regrouped chain with $l=2$ and $p=3$

An example of such regrouping is shown in Fig. 4.3 for the choice $l=2$ and $p=3$. The sites are represented by ellipses, while the interactions are the lines connecting the ellipses. Due to the frustration-free condition and the translation invariance of the Hamiltonians,

the ground states of H and $\tilde{H}$ coincide on the sites $\{p+1,\ldots,N\}$. By construction, each $h_{i,\ldots,i+l}$ term appears at most twice in $\tilde{H}$, so we obtain the inequality

$$\tilde{H} \leq 2H. \tag{4.31}$$

In Fig. 4.3, only the interaction lines that do not cross any dashed rectangles appear twice in the regrouped Hamiltonian. Furthermore, each index i on the regrouped chain corresponds to p sites on the original chain, so any local Hamiltonian $\tilde{h}_{i',(i+1)'}$ acts on $2p$ spins on the original chain. Thus, the local gap ϵ_{2p} satisfies

$$\tilde{h}_{i',(i+1)'} \geq \epsilon_{2p}(\mathbb{1} - G_{pi'+1,\ldots,p(i'+2)}). \tag{4.32}$$

The ground space projections of the terms that are summed up in Eq. (4.30) can overlap on maximum p sites, so we recover that, if the following condition analogously to Eq. (4.21) and Eq. (4.27) holds:

$$\|G_{p+1,\ldots,p(i'+1)}G_{pi'+1,\ldots,p(i'+2)} - G_{p+1,\ldots,p(i'+2)}\| \leq \gamma_p < \frac{1}{\sqrt{2}} \qquad \forall i' \in \{1,\ldots,m-2\}, \tag{4.33}$$

then the spectral gap satisfies [28, Thm. 3]

$$\epsilon \geq \frac{\epsilon_{2p}}{2}(1 - \sqrt{2}\cdot\gamma_p)^2. \tag{4.34}$$

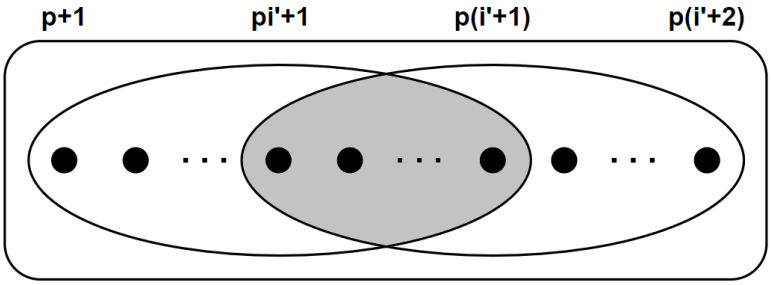

Figure 4.4.: Schematic representation of the left-hand side of Eq. (4.33)

A schematic sketch of the left-hand side of Eq. (4.33) is shown in Fig. 4.4, where the gray area corresponds to the region consisting of p sites, where the ground space projectors overlap. It is useful to emphasize the difference in the approaches that lead to the conditions presented in Eq. (4.27) and Eq. (4.33). In Eq. (4.27) the Hamiltonian being studied has an interaction length $l+1$ and the ground spaces overlap on at most l sites. On the other hand, the Hamiltonian leading to the condition in Eq. (4.33) is a sum of two-body terms on a regrouped chain, where the ground spaces overlap on p sites on the original chain.

4.2.2. Application to parent Hamiltonians of injective MPS

Now, with the conditions given above, we first calculate bounds of the form as in Eq. (4.33) for frustration-free Hamiltonians that possess a unique ground state in the form of an injective MPS generated by the tensor M with injectivity length l, and the Hamiltonians have the form as in Eq. (3.30) with local terms in Eq. (3.29) after blocking $p > l$ sites together. We start by reducing the problem of projectors to a problem of states, where we follow [10]. To visually simplify the calculations, we write $\|G_{b+p}G_{p+c} - G_{b+p+c}\|$ instead of the left hand side of Eq. (4.33). In this proof, the subscript denotes the number of sites on which an operator is acting. Since the projections commute if their domains completely overlap, we can write

$$(G_{b+p} \otimes \mathbb{1}_c)(\mathbb{1}_b \otimes G_{p+c}) - G_{b+p+c} = (G_{b+p} \otimes \mathbb{1}_c - G_{b+p+c})(\mathbb{1}_b \otimes G_{p+c} - G_{b+p+c}). \quad (4.35)$$

Each factor is thus a Hermitian projector, and the two terms do not necessarily commute. To simplify the notation, let us write $P = G_{b+p} \otimes \mathbb{1}_c - G_{b+p+c}$ and $Q = \mathbb{1}_b \otimes G_{p+c} - G_{b+p+c}$. The norm of PQ is thus the norm of the right hand side of Eq. (4.35) which is the quantity we want to bound to obtain an estimate for the ground state gap:

$$\|PQ\| = \sup_{|\Omega\rangle} \frac{\|PQ|\Omega\rangle\|}{\||\Omega\rangle\|} = \sup_{|\Omega\rangle} \sqrt{\frac{\langle\Omega|(PQ)^\dagger PQ|\Omega\rangle}{\langle\Omega|\Omega\rangle}} = \sup_{|\Omega\rangle} \sqrt{\frac{\langle\Omega|QPQ|\Omega\rangle}{\langle\Omega|\Omega\rangle}} \quad (4.36)$$

for $|\Omega\rangle \in (\mathbb{C}^d)^{\otimes b+p+c} \setminus \{0\}$. Let $|\Psi\rangle$ be in the range of Q, i.e. $|\Psi\rangle \in (\mathbb{C}^d)^{\otimes b} \otimes \mathcal{G}_{p+c}$ with $|\Psi\rangle \perp \mathcal{G}_{b+p+c}$. Since $\operatorname{Im} Q \subseteq (\mathbb{C}^d)^{\otimes b+p+c}$, we have

$$\sup_{|\Omega\rangle} \sqrt{\frac{\langle\Omega|QPQ|\Omega\rangle}{\langle\Omega|\Omega\rangle}} \geq \sup_{|\Psi\rangle \in \operatorname{Im} Q \setminus \{0\}} \sqrt{\frac{\langle\Psi|P|\Psi\rangle}{\langle\Psi|\Psi\rangle}}, \quad (4.37)$$

but if we set $|\Psi\rangle = Q|\Omega\rangle$, then

$$\langle\Psi|\Psi\rangle = \langle\Omega|Q|\Omega\rangle \leq \langle\Omega|\Omega\rangle, \quad (4.38)$$

thus

$$\|PQ\| = \sup_{|\Omega\rangle} \sqrt{\frac{\langle\Omega|QPQ|\Omega\rangle}{\langle\Omega|\Omega\rangle}} = \sup_{|\Psi\rangle \in \operatorname{Im} Q \setminus \{0\}} \sqrt{\frac{\langle\Psi|P|\Psi\rangle}{\langle\Psi|\Psi\rangle}}. \quad (4.39)$$

Similarly, let $|\Phi\rangle$ be in the range of P, then $\langle\Phi|\Phi\rangle \cdot P \geq |\Phi\rangle\langle\Phi|$, and thus

$$\|PQ\| \geq \sup_{\substack{|\Psi\rangle \in \operatorname{Im} Q \setminus \{0\} \\ |\Phi\rangle \in \operatorname{Im} P \setminus \{0\}}} \sqrt{\frac{\langle\Psi|\Phi\rangle\langle\Phi|\Psi\rangle}{\langle\Psi|\Psi\rangle\langle\Phi|\Phi\rangle}} = \sup_{\substack{|\Psi\rangle \in \operatorname{Im} Q \setminus \{0\} \\ |\Phi\rangle \in \operatorname{Im} P \setminus \{0\}}} \frac{|\langle\Phi|\Psi\rangle|}{\||\Phi\rangle\| \cdot \||\Psi\rangle\|}. \quad (4.40)$$

However, the choice $|\Phi\rangle = P|\Psi\rangle$ saturates this inequality, so

$$\|PQ\| = \sup_{\substack{|\Psi\rangle\in \mathrm{Im}\, Q\setminus\{0\} \\ |\Phi\rangle\in \mathrm{Im}\, P\setminus\{0\}}} \frac{|\langle\Phi|\Psi\rangle|}{\||\Phi\rangle\| \cdot \||\Psi\rangle\|}. \tag{4.41}$$

We now deviate from the original proof given in [10], because the graphical notation enables us to provide a simpler way of obtaining the same result. Since the vectors $|\Psi\rangle$ and $|\Phi\rangle$ are set to be in the range of G_{b+p} and G_{p+c}, respectively, we can represent them in the graphical notation as

$|\Phi\rangle =$ 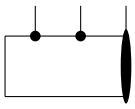 , $\qquad |\Psi\rangle =$ 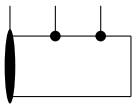 , (4.42)

where the non-lettered nodes represent the blockings of the MPS tensor M on the regrouped chain. The objects $\hat{\Psi}$ and $\hat{\Phi}$ denote d^b-and d^c-tuples of $D \times D$ matrices, with the additional constraint that $|\Psi\rangle$ and $|\Phi\rangle$ are orthogonal to the $b + p + c$-site ground space. When calculating their overlap, the b and c indices are being summed over, so we can utilize the tensor network notation to rewrite sums of inequalities of the form as in Eq. (3.27), since the middle of the overlap is the transfer matrix on p sites:

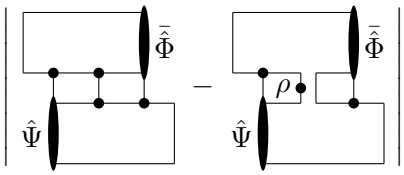 $\leq a(p) \sum_{i,j} \|M^i \hat{\Phi}^j\|_\rho \|\hat{\Psi}^i M^j\|_\rho,$ (4.43)

where $i \in \{1, \ldots, d^b\},\ j \in \{1, \ldots, d^c\}$. Similarly, one can calculate the square of the norms on the right hand side by using the identities given in Eq. (3.21) for the left and right fixed points of the transfer matrix:

$\sum_{i,j} \|M^i \hat{\Phi}^j\|_\rho^2 =$ 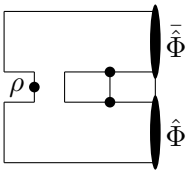 $= \sum_j \|\hat{\Phi}^j\|_\rho^2$ (4.44)

$\sum_{i,j} \|\hat{\Psi}^i M^j\|_\rho^2 =$ 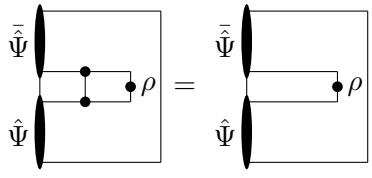 $= \sum_i \|\hat{\Psi}^i\|_\rho^2.$ (4.45)

By utilizing the inequality in Eq. (3.28) for each term of the sums and the fact that $a_-(p)$ is monotonously increasing, we arrive at

$$\sum_j \|\hat{\Phi}^j\|_\rho^2 \leq \frac{1}{a_-(b+p)} = \frac{\||\Phi\rangle\|^2}{a_-(b+p)} \leq \frac{\||\Phi\rangle\|^2}{a_-(p)} \tag{4.46}$$

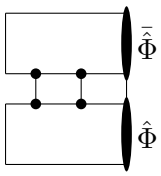

Analogously, we have $\sum_i \|\hat{\Psi}^i\|_\rho^2 \leq \||\Psi\rangle\|^2/a_-(p)$. After using the Cauchy-Schwarz inequality on the right-hand side of Eq. (4.43), the substitution of the previous results, i.e.,

$$\sum_{i,j} \|M^i\hat{\Phi}^j\|_\rho^2 \leq \frac{\||\Phi\rangle\|^2}{a_-(p)}, \qquad \sum_{i,j} \|\hat{\Psi}^i M^j\|_\rho^2 \leq \frac{\||\Psi\rangle\|^2}{a_-(p)}, \tag{4.47}$$

leads to the inequality

$$\left| \quad - \quad \right| \leq \frac{a(p)}{a_-(p)} \||\Phi\rangle\| \cdot \||\Psi\rangle\|. \tag{4.48}$$

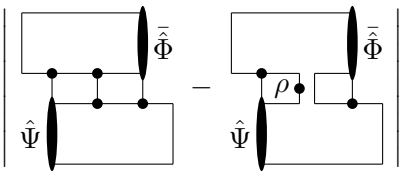

By the triangle inequality we then have

$$|\langle\Phi|\Psi\rangle| \leq \left| \quad \right| + \frac{a(p)}{a_-(p)} \||\Phi\rangle\| \cdot \||\Psi\rangle\|. \tag{4.49}$$

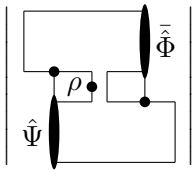

Now, the aim is to exploit the orthogonality of $|\Phi\rangle$ and $|\Psi\rangle$ to the $b+p+c$-site ground space to bound the first term on the right-hand side of Eq. (4.49), which can be viewed as the ρ-scalar product of two $D \times D$ matrices, i.e. of the form $\langle\Delta_\Phi|\Delta_\Psi\rangle_\rho$ with

$$|\Delta_\Psi\rangle = \quad , \qquad |\Delta_\Phi\rangle = \quad . \tag{4.50}$$

We take $|\chi\rangle \in \mathcal{G}_{b+p+c}$, i.e., an injective MPS on $b+p+c$ sites with a non-trivial boundary $\hat{\chi} \in \mathcal{M}_D$,

$$|\chi\rangle = \quad , \tag{4.51}$$

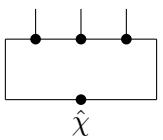

such that $\langle\Phi|\chi\rangle = \langle\Psi|\chi\rangle = 0$. Due to the orthogonality and the first identity in Eq. (3.21), Eq. (3.27) reduces to

$$|\langle\hat{\chi}|\Delta_\Psi\rangle_\rho| = \left| \right| \leq a(p) \sum_{b,c} \|M^b \hat{\chi} M^c\|_\rho \cdot \|\hat{\Psi}^b M^c\|_\rho. \tag{4.52}$$

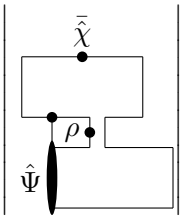

The sum of norms containing $\hat{\chi}$ is calculated again with the identities in Eq. (3.21):

$$\sum_{b,c} \|M^b \hat{\chi} M^c\|_\rho^2 = \quad = \quad = \|\hat{\chi}\|_\rho^2. \tag{4.53}$$

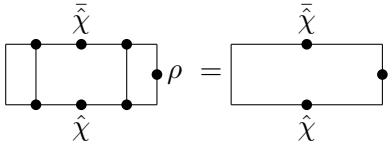

As a consequence, we have $|\langle\hat{\chi}|\Delta_\Psi\rangle_\rho| \leq a(p) \cdot a_-(p)^{-1/2} \|\hat{\chi}\|_\rho \cdot \||\Psi\rangle\|$. Since this inequality holds for any $D \times D$ matrix $\hat{\chi}$, we have

$$\||\Delta_\Psi\rangle\|_\rho \leq \frac{a(p)}{\sqrt{a_-(p)}} \||\Psi\rangle\|, \qquad \||\Delta_\Phi\rangle\|_\rho \leq \frac{a(p)}{\sqrt{a_-(p)}} \||\Phi\rangle\|, \tag{4.54}$$

where we analogously included the relation for the ρ-norm of $|\Delta_\Phi\rangle$ as well. By using the triangle- and Cauchy-Schwarz inequalities we arrive at an explicit upper bound on the overlaps:

$$|\langle\Phi|\Psi\rangle| \leq |\langle\Delta_\Phi|\Delta_\Psi\rangle| + \frac{a(p)}{a_-(p)} \||\Phi\rangle\| \cdot \||\Psi\rangle\| \leq \frac{a(p)\,(1+a(p))}{a_-(p)} \||\Phi\rangle\| \cdot \||\Psi\rangle\|, \tag{4.55}$$

so the left hand side of Eq. (4.33) is bounded by $a(p) \cdot (1 + a(p))/a_-(p)$. We now use Eq. (3.26), that is $a(p) \leq D^2 \lambda^p$, where D is the bond dimension and λ is the second largest eigenvalue of the transfer matrix. We furthermore use Eq. (3.28) to explicitly write a lower bound for $a_-(p)$, arriving at

$$\|(G_{b+p} \otimes \mathbb{1}_c)(\mathbb{1}_b \otimes G_{p+c}) - G_{b+p+c}\| \leq D^2 \lambda^p \, \frac{1 + D^2 \lambda^p}{1 - D^2 \lambda^p}. \tag{4.56}$$

Since the right-hand side of the inequality decays exponentially with p, one can always find a positive integer p such that the right hand side of Eq. (4.56) is smaller than $1/\sqrt{2}$. Consequently, the parent Hamiltonian of an injective MPS is always gapped, and the spectral gap ϵ has a lower bound

$$\epsilon \geq \frac{\epsilon_{2p}}{2} \left(1 - \sqrt{2} D^2 \lambda^p \, \frac{1 + D^2 \lambda^p}{1 - D^2 \lambda^p}\right)^2, \tag{4.57}$$

where we explicitly used Eq. (4.34).
Similarly, instead of basing the method on Eq. (4.34), providing a bound on γ_l given in Eq. (4.28) might provide better bounds on the spectral gap, which is then given by

$$\epsilon \geq \frac{\epsilon_{l+1}}{l}\left(1-\sqrt{l+1}D^2\lambda^l\,\frac{1+D^2\lambda^l}{1-D^2\lambda^l}\right)^2. \tag{4.58}$$

4.2.3. Application to systems with ground state degeneracies

It is possible to extend the arguments given before to Hamiltonians which have a finite number of ground states in the thermodynamic limit, with all of them being injective matrix product states, such that their overlap vanishes if the system size tends to infinity. The idea of the extension is to relate the left hand side of Eq. (4.33) (where G now projects onto the whole ground space) to simpler bounded terms. Below we sketch the most important steps to arrive at the bound given in [28, Lemma 11.ii)].
Let $\{\mathcal{G}_p^\alpha\}_{\alpha=1}^n$ be the range of the p-site orthogonal projectors $\{G_p^\alpha\}_{\alpha=1}^n$ onto the distinct ground spaces labeled by α. Let $o_{\alpha\beta}^{(p)}$ be the overlaps of the respective ground spaces, $o_{\alpha\beta}^{(p)} \coloneqq \mathcal{O}(\mathcal{G}_p^\alpha, \mathcal{G}_p^\beta)$ for $\alpha \neq \beta$ and $o_{\alpha\alpha}^{(p)} \coloneqq 0$ for all $\alpha \in \{1,\ldots,n\}$. Choose p large enough such stat $o_{\alpha\beta}^{(p)} < 1/(2(n-1))$. We then define

$$\delta_p = \frac{\|o^{(p)}\|}{1-\|o^{(p)}\|}, \tag{4.59}$$

where $o^{(p)} = (o_{\alpha\beta}^{(p)})$ is the symmetric matrix containing all overlaps. With the help of an auxiliary result [28, Lemma 11.i)], which provides an upper bound on the quantity

$$\left\|\sum_{\alpha=1}^n G_p^\alpha - G_p\right\| \leq \frac{\delta_p}{1-\delta_p}, \tag{4.60}$$

the triangle inequality and further previous results in [10] and [28] can be utilized to prove that

$$\|(G_{b+p}\otimes\mathbb{1}_c)(\mathbb{1}_b\otimes G_{p+c}) - G_{b+p+c}\| \leq \frac{4\delta_p}{(1-\delta_p)^2} + \sum_{\alpha=1}^n D_\alpha^2\lambda_\alpha^p\,\frac{1+D_\alpha^2\lambda_\alpha^p}{1-D_\alpha^2\lambda_\alpha^p}, \tag{4.61}$$

where D_α is the bond dimension of the injective MPS labeled by α, and λ_α is the absolute value of the second largest eigenvalue of its transfer matrix. We present the sketch of the proof of this expression in Appendix A.1, since it would shift the emphasis of the section and the proof itself uses the same steps and language as [28]. However, some details of the proof are necessary to later optimize the methods to bound the ground state gap for some given models. Since both of the terms on the right hand side decrease with p, there exists a finite length p such that a non-trivial lower bound on the spectral gap of the

Hamiltonian is obtained, where γ_p from Eq. (4.33) is bounded from above by the right hand side by Eq. (4.61). The first term of the right hand side can be further bounded if we only know the maximal overlap $o_{\max}^{(p)}$ between any two ground spaces on p sites. The norm of the overlap matrix is then bounded from above by $(n-1)o_{\max}^{(p)}$, thus

$$\delta_p \leq \frac{(n-1)o_{\max}^{(p)}}{1-(n-1)o_{\max}^{(p)}}. \tag{4.62}$$

Consequently, we can further estimate the norm on the left hand side of Eq. (4.61) by

$$\|(G_{b+p}\otimes \mathbb{1}_c)(\mathbb{1}_b\otimes G_{p+c}) - G_{b+p+c}\| \leq \frac{1}{(1-2(n-1)o_{\max}^{(p)})^2} - 1 + \sum_{\alpha=1}^{n} D_\alpha^2 \lambda_\alpha^p \frac{1+D_\alpha^2\lambda_\alpha^p}{1-D_\alpha^2\lambda_\alpha^p}. \tag{4.63}$$

This expression provides a corrected estimate in contrast to the one found in [28, Prop. 12], since it accounts for the $1/(1-\delta_p)$ factor that is missing from that estimation. The corrected bound in Eq. (4.63) is however less strict, since $1/(1-\delta_p)$ is larger than one due to Eq. (4.62).

5. Comparison of the Knabe and martingale method for already existing models

5.1. Witten's conjugation

Witten's conjugation [30] creates new Hamiltonians from supersymmetric quantum mechanical Hamiltonians, deforming them in a way such that the ground state degeneracies remain invariant. This construction was utilized by Wouters et al. [18] for spin chains with frustration-free Hamiltonians, i.e., for models where the energy is minimized locally. The aim of this section is to introduce the notion of Witten's conjugation for spin chains and discuss its most important properties along the lines of [18].

The setup consists of a one-dimensional lattice with open boundary conditions, where a finite-dimensional Hilbert space is assigned to each lattice site. The Hamiltonian is restricted to nearest-neighbor interactions, so for N sites it takes the form:

$$H = \sum_{j=1}^{N-1} H_{j,j+1} = \sum_{j=1}^{N-1} L_{j,j+1}^{\dagger} L_{j,j+1}, \tag{5.1}$$

where j and $j+1$ denote the individual lattice sites and the existence of L ensures that the local terms of the Hamiltonian are positive semidefinite, so for each vector $|\psi\rangle$ in the two-site Hilbert space of sites j and $j+1$ the expectation value of the local Hamiltonian $\langle\psi|H_{j,j+1}|\psi\rangle$ is non-negative.

The Hamiltonian is constructed in a way such that each $L_{j,j+1}$ operator evaluated on any ground state yields zero as a result. With the Hamiltonian being frustration-free, the global ground states are exactly the zero-energy states.

It is useful to denote global operators by capital letters and single-site operators by lower case letters. The deformation is given by an invertible operator M_j acting non-trivially on a single site j:

$$M_j = \mathbb{1} \otimes \cdots \otimes \mathbb{1} \otimes m_j \otimes \mathbb{1} \otimes \cdots \otimes \mathbb{1}, \tag{5.2}$$

together with nearest-neighbor positive definite operators $C_{j,j+1}$. The deformed, or conjugated, Hamiltonian $\tilde{H}$ is given by

$$\tilde{H} = \sum_{j=1}^{N-1} \tilde{H}_{j,j+1} = \sum_{j=1}^{N-1} \tilde{L}_{j,j+1}^{\dagger} C_{j,j+1} \tilde{L}_{j,j+1}, \tag{5.3}$$

where $\tilde{L}_{j,j+1}$ is

$$\tilde{L}_{j,j+1} = M_j M_{j+1} L_{j,j+1} M_{j+1}^{-1} M_j^{-1}. \tag{5.4}$$

The locality of the individual terms in the deformation ensures the local nature of the deformed Hamiltonian. In order to simplify the deformation operators, we can always choose a single-site local basis transformation to transform it further without changing the spectrum of the Hamiltonian.

If the original Hamiltonian given in Eq. (5.1) has ground states $\{|\psi_i\rangle\}_{i=1}^{d}$, then the conjugated Hamiltonian's only ground states will be $\{\prod_j M_j|\psi_i\rangle\}_{i=1}^{d}$, thus, the ground state degeneracy of the Hamiltonian remains invariant under the deformation.

The procedure described in this section was utilized to relate the classical Ising chain to the frustration-free line to the Kitaev chain [31] and to the Peschel-Emery line [32] of the axial next-nearest neighbour Ising model [33], for different choices of $C_{j,j+1}$. The next section will focus on deformations of the Potts clock model via Witten's conjugation, following [18].

5.2. Deformed clock models

One can consider the $\mathbb{Z}_d$-clock model to be a generalization of the Ising model, where the model is characterized by the $\mathbb{Z}_d$ symmetry instead of the $\mathbb{Z}_2$ symmetry of the conventional transverse-field Ising model. For the setup a d-dimensional local Hilbert space is considered on each lattice site. The clock algebra can be specified with the single-site operators σ and τ that satisfy the following relations:

$$\sigma^d = \tau^d = \mathbb{1}, \quad \sigma^{d-1} = \sigma^{\dagger}, \quad \tau^{d-1} = \tau^{\dagger}, \quad \sigma\tau = \omega\tau\sigma, \tag{5.5}$$

where $\omega = \exp\left(\frac{2\pi i}{d}\right)$ denotes the d-th root of unity. Let $\{|\sigma, i\rangle\}_{i=0}^{d-1}$ and $\{|\tau, i\rangle\}_{i=0}^{d-1}$ denote the eigenstates of σ and τ, respectively. The eigenvalue equations of these local operators are the following:

$$\begin{aligned} \sigma|\sigma, i\rangle &= \omega^i|\sigma, i\rangle, \quad \tau|\sigma, i\rangle = |\sigma, i+1\rangle, \\ \sigma|\tau, i\rangle &= |\tau, i-1\rangle, \quad \tau|\tau, i\rangle = \omega^i|\tau, i\rangle, \end{aligned} \tag{5.6}$$

where the addition is taken modulo d. If one were to describe the Ising model in this formalism, τ would correspond to the Pauli matrix σ^Z, and σ to σ^X. Then it is straightforward to check that the conditions given in Eq. (5.5)-(5.6) hold for $d = 2$.

The local Hamiltonian of the clock model is given by

$$H_{j,j+1} = 2 - \sigma_j \sigma_{j+1}^\dagger - \sigma_j^\dagger \sigma_{j+1}, \tag{5.7}$$

which corresponds to the choice $L_{j,j+1} = \sigma_j - \sigma_{j+1}$. The Hamiltonian is thus positive semidefinite with its lowest eigenvalue being 0, and it is frustration-free: the ground states of the global Hamiltonian can be written as products of the σ_j-eigenstates:

$$|\psi_i\rangle = \bigotimes_j |\sigma, i\rangle_j, \tag{5.8}$$

thus the ground state degeneracy of the $\mathbb{Z}_d$-clock model is d.

It is straightforward to check either with Knabe's argument [9] or the martingale method [28] that the undeformed clock model defined on an open chain has a spectral gap in the thermodynamic limit. The ground states in Eq. (5.8) build an orthonormal basis, thus any pair of two-body ground space projections $G_{j,j+1}$ commute. Consequently, the auxiliary frustration-free Hamiltonian $\tilde{H} = \sum_j \mathbb{1} - G_{j,j+1}$ with ground states given in Eq. (5.8) has a spectral gap lower bounded by 1.

The following subsections are going to introduce specific deformations of the clock model that resemble already existing models. Besides invertibility, the authors also require the deformation to respect the initial $\mathbb{Z}_d$-symmetry of the system, i.e. the single-site deformation matrix m_j has to be diagonal in the eigenbasis of τ. Consequently, the deformed ground states $\{|\tilde{\psi}_i\rangle\}$ are the following:

$$|\tilde{\psi}_i\rangle = \prod_j M_j |\psi_i\rangle = \bigotimes_j m_j |\sigma, i\rangle_j. \tag{5.9}$$

As the deformed ground states are product states, they can be straightforwardly written in the formalism of MPS with bond dimension 1. To simplify the notation, the τ-eigenstates will be written as $\{|i\rangle\}_{i=0}^{d-1}$. From Eq. (5.6) the σ-eigenstates can be written as the following linear combination of the τ-eigenstates:

$$|\sigma, i\rangle = \frac{1}{\sqrt{d}} \sum_{k=0}^{d-1} \omega^{i \cdot k} |k\rangle, \tag{5.10}$$

which allows for a translation-invariant MPS-representation of the undeformed N-site ground states

$$|\psi_i\rangle = \sum_{k_1,\ldots k_N=0}^{d-1} \mathrm{Tr}(A_i^{k_1} \ldots A_i^{k_N}) |k_1 \ldots k_N\rangle, \qquad A_i^{k_j} = \frac{1}{\sqrt{d}} \omega^{i \cdot k_j} \tag{5.11}$$

By taking the deformation given in Eq. (5.9) into consideration together with the fact that m_j is required to be diagonal in the chosen basis, we arrive at

$$|\tilde{\psi}_i\rangle = \sum_{k_1,\dots k_N=0}^{d-1} \mathrm{Tr}(\tilde{A}_i^{k_1}\dots\tilde{A}_i^{k_N})|k_1\dots k_N\rangle, \qquad \tilde{A}_i^{k_j} = \frac{1}{\sqrt{d}}\,\omega^{i\cdot k_j}(m_j)_{k_jk_j}. \tag{5.12}$$

In order to represent the whole ground space, it is also possible to build a block-injective MPS consisting of the following $(d-1)\times(d-1)$ diagonal matrices with $k_j \in \{0,\dots,d-1\}$:

$$N^{k_j} = \mathrm{diag}(\tilde{A}_0^{k_j},\dots,\tilde{A}_{d-1}^{k_j}) = \mathrm{diag}\left(\frac{1}{\sqrt{d}}(m_j)_{k_jk_j}, \frac{1}{\sqrt{d}}\omega^{k_j}(m_j)_{k_jk_j},\dots,\frac{1}{\sqrt{d}}\omega^{(d-1)k_j}(m_j)_{k_jk_j}\right). \tag{5.13}$$

As the deformed ground states are product states, the intersection property given in Eq. (3.31) holds, and thus $\|(G^{(i)}_{b+p}\otimes\mathbb{1}_c)(\mathbb{1}_b\otimes G^{(i)}_{p+c}) - G^{(i)}_{b+p+c}\| = 0$, where $G^{(i)}_p$ is the orthogonal projector that projects onto the space spanned by a single ground state $|\tilde{\psi}_i\rangle$ on p sites. As a consequence, it becomes simpler to utilize the martingale method, as the bound for the spectral gap only depends on the overlap between the individual ground state spaces. As defined in Eq. (3.35) and in section 4.2, the overlap o_{ij} is given by

$$o_{ij} = \sup_{\substack{|\phi_i\rangle\in\mathrm{span}(|\tilde{\psi}_i\rangle)\\ |\phi_j\rangle\in\mathrm{span}(|\tilde{\psi}_j\rangle)}} \frac{|\langle\phi_i|\phi_j\rangle|}{\||\phi_i\rangle\|\cdot\||\phi_j\rangle\|} = |\langle\tilde{\psi}_i|\tilde{\psi}_j\rangle| \tag{5.14}$$

for $i\neq j$. The overlaps are functions of the parameters that specify the deformation M. Furthermore, the p-site overlaps are simply the p-th powers of the one-site overlaps, so they are decreasing functions of p. Invertibility of the deformation implies that the ground states are distinct even in the thermodynamic limit. As a consequence, the necessary step to prove the existence of the ground state gap in a deformed clock model is to find a large enough p such that the overlaps become so small that the right hand side of Eq. (4.61) becomes small enough such that it will satisfy Eq. (4.27) or Eq. (4.33). More specifically, by the inequality

$$\|(G_{b+p}\otimes\mathbb{1}_c)(\mathbb{1}_b\otimes G_{p+c}) - G_{b+p+c}\| \leq \frac{4\delta_p}{(1-\delta_p)^2} = \frac{4\|o^{(p)}\|\cdot(1-\|o^{(p)}\|)}{(1-2\|o^{(p)}\|)^2} \tag{5.15}$$

where in the equality we used $\delta_p = \|o^{(p)}\|/(1-\|o^{(p)}\|)$, we obtain the following bound on the spectral gap:

$$\epsilon \geq \frac{\epsilon_{2p}}{2}\left(1 - \frac{4\sqrt{2}\|o^{(p)}\|\cdot(1-\|o^{(p)}\|)}{(1-2\|o^{(p)}\|)^2}\right)^2. \tag{5.16}$$

In the following subsections, we will discuss models obtained by specific deformations.

5.2.1. $\mathbb{Z}_3$ models

$\mathbb{Z}_3$-XY model

First consider the case $d = 3$ with a simple deformation, where the additional degree of freedom is set to unity:

$$C_{j,j+1} = \mathbb{1}. \tag{5.17}$$

The deformation matrix for a single site is given by

$$m_j = \begin{pmatrix} 1 & & \\ & r & \\ & & r^2 \end{pmatrix}, \tag{5.18}$$

where r is set to be positive and real. The Hamiltonian resulting from the deformation is then

$$\tilde{H}_{j,j+1} = \epsilon - \left[\left(1 + b\tau_j + b\tau_j^\dagger\right) \sigma_j^\dagger \sigma_{j+1} \left(1 + b\tau_{j+1} + b\tau_{j+1}^\dagger\right) + \frac{f}{2} \left(\tau_j + \tau_{j+1}\right) + \text{h.c.} \right], \tag{5.19}$$

where the parameters are

$$f = \frac{6(1 - r^6)}{(r^3 + 2)^2}, \qquad b = \frac{r^3 - 1}{r^3 + 2}, \qquad \epsilon = \frac{6(r^6 + 2)}{(r^3 + 2)^2}. \tag{5.20}$$

The choice of ϵ ensures that the lowest eigenvalue of the system remains zero. This deformed Hamiltonian corresponds to the $\mathbb{Z}_3$-generalization of the frustration-free line of the transverse-field $\mathbb{Z}_2$-XY model [18], studied beforehand by Iemini et al. [34].

In [18] it was proven with the Knabe method [9] that the system given by the Hamiltonian in Eq. (5.19) is gapped for the parameter range $0.5695 \lesssim r \lesssim 1.7560$ in the thermodynamic limit.

Here, we utilize the martingale method to show that the model is gapped for all $0 < r < \infty$. The single-site overlaps in Eq. (5.14) of the ground spaces are given by

$$o_{ij}^{(1)} = \frac{|r^2 - 1|}{\sqrt{r^4 + r^2 + 1}} =: o^1(r), \tag{5.21}$$

for all $i, j \in \{1, 2, 3\}$, $i \neq j$, and we also have $o^p(r) = (o^{(1)}(r))^p$. The norm of the matrix defined by the overlaps (with the diagonal terms being set to zero) is then $\|o^{(1)}\| = 2o^{(1)}(r)$, so we have

$$\delta_p = \frac{2o^p(r)}{1 - 2o^p(r)}. \tag{5.22}$$

By requiring that the right-hand side of Eq. (5.15) is bounded by $1/\sqrt{2}$ according to Eq. (4.33), the martingale method proves the existence of the gap if p is large enough such that the following holds:

$$\left(\frac{|r^2-1|}{\sqrt{r^4+r^2+1}}\right)^p < \frac{1}{4}\left(1-\sqrt{2-\sqrt{2}}\right). \tag{5.23}$$

This inequality implies that for any given $0 < r < \infty$ there exists an integer $p > 1$ such that Eq. (5.23) is satisfied, thus the spectral gap of the Hamiltonian given in Eq. (5.19) is bounded from below by

$$\epsilon \geq \frac{\epsilon_{2p}}{2}\left(1-\frac{8\sqrt{2}o^p(r)(1-2o^p(r))}{(1-4o^p(r))^2}\right)^2, \tag{5.24}$$

where ϵ_{2p} is the gap of the $2p$-site local Hamiltonian. Consequently, the Hamiltonian is gapped in the parameter region $0 < r < \infty$.

By utilizing Eq. (5.24), the smallest integer to provide bounds on the gap outside the parameter range given in [18] is $p = 5$, which requires the diagonalization of a 10-site Hamiltonian. Since the local Hamiltonian in Eq. (5.19) is a sparse matrix, it is possible to utilize a Lánczos method for sparse Hermitian matrices [35]. The algorithm converges in the whole observed parameter interval for the default tolerance, which is the machine precision. The Lánczos-diagonalization of the 10-site Hamiltonian requires roughly the same amount of computation time as the diagonalization of the $m = 7$-site projector Hamiltonian necessary for Knabe's method. The numerically obtained Knabe and martingale bounds for $1 \leq r \leq 2$ are shown in Fig. 5.1a. The extended parameter region where an estimate is obtained by the martingale method is $0.5681 \lesssim r \lesssim 1.7605$. Furthermore, the martingale method provides an improved bound in comparison to the Knabe method in the parameter interval $1.2642 \lesssim r \lesssim 1.7261$. Even though the martingale method provides an estimate for the gap in a larger parameter region, Knabe's method provides better bounds near the point where it stops detecting the gap. This behavior is plotted in Fig. 5.1b in the interval $1.72 \leq r \leq 1.77$.

In addition, the Knabe bounds are substantially more powerful in the regions in the parameter space, where the overlaps of the ground spaces are small. This can be explained with the $1/2$ scaling factor for the martingale method in Eq. (5.24).

To combat this, it is possible to utilize Eq. (4.27) as well, where for $l = 1$ there is no scaling factor in front of the expression for the bound. In addition to that, for arbitrary positive integers l the condition for the existence of the gap for a given r obtained beforehand in Eq. (5.23) then changes to

$$\left(\frac{|r^2-1|}{\sqrt{r^4+r^2+1}}\right)^l < \frac{1}{4} - \frac{\sqrt{l+1}}{4\sqrt{l+1+\sqrt{l+1}}}, \tag{5.25}$$

and the bound on the gap changes correspondingly as

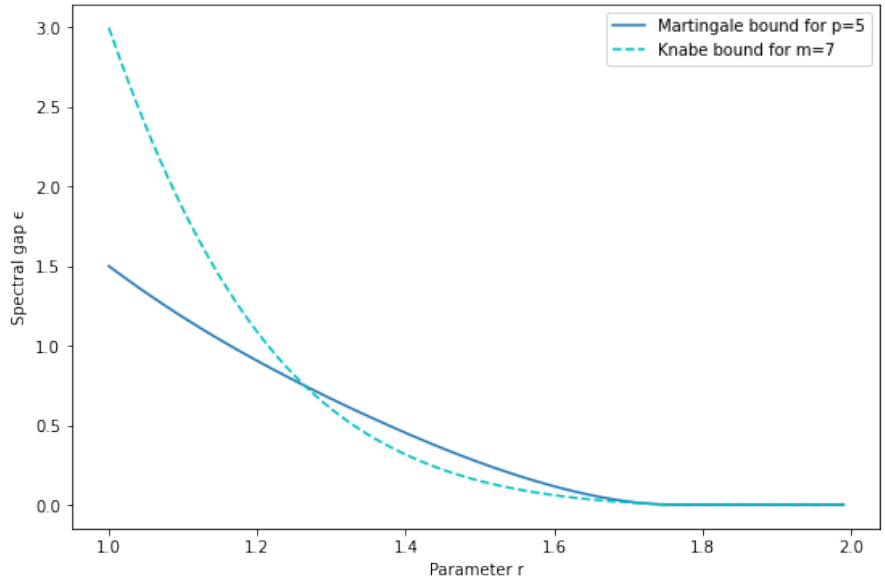

(a) Comparison in the range $1 \leq r \leq 2$

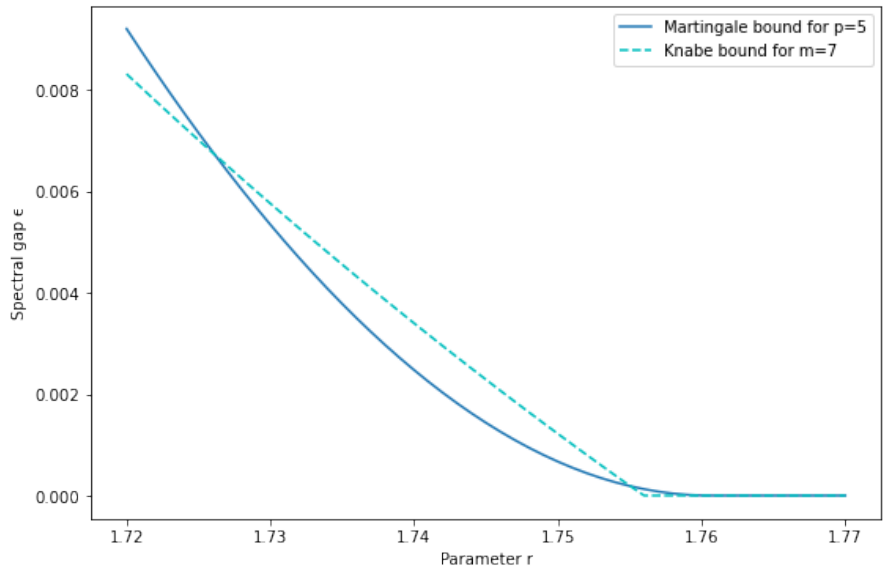

(b) Comparison in the range $1.72 \leq r \leq 1.77$

Figure 5.1.: Comparison of the Knabe and martingale ($p = 5$) bound for the deformed $\mathbb{Z}_3$-XY model

$$\epsilon \geq \frac{\epsilon_{l+1}}{l}\left(1-\frac{8\sqrt{l+1}o^l(r)(1-2o^l(r))}{(1-4o^l(r))^2}\right)^2. \tag{5.26}$$

As a consequence, one can further enlarge the parameter region where an explicit estimate for the spectral gap is found by using the same computational resources.

Due to the $1/l$-dependency of the prefactor in the bound, this expression gives less strict bounds for increasing l. By solving the inequality given in Eq. (5.25) we conclude that the parameter interval, where a lower bound on the gap is obtained, is extended to $0.4775 \lesssim r \lesssim 1/0.4775 \approx 2.0944$ for $l = 9$.

In Fig. 5.2 we show the best martingale bounds computed for either $p = 5$ according to Eq. (5.24) or $l = 1$ or $l = 9$ according to Eq. (5.26) in comparison with the Knabe bound for $m = 7$ for the values $1 \leq r \leq 2.1$. For $l \in \{2, \ldots, 8\}$, the bounds obtained are smaller than the bounds shown in the figure for the whole observed parameter interval, so they are not displayed in the plot. The $l = 9$-martingale method provides the largest computed bound from around the point $r \approx 1.67$, so we also plot its behavior in Fig. 5.2b. In conclusion, the martingale bound now provides a better gap in the range $1.2642 \lesssim r \lesssim 2.0944$.

The estimate for $l = 1$ yields a better estimate only on an extremely small interval compared to $p = 5$. For small l or p, it is possible to optimize the martingale method due to the simplicity of the model. As previously discussed in Section 4.2, the expression in Eq. (5.26) was obtained by first bounding the quantity $\|X_p - G_p\|$ where $X_p = \sum_{\alpha=1}^{n} G_p^\alpha$ and then by utilizing previous results in [28] alongside the Cauchy-Schwarz- and triangle inequalities. The simplicity of the ground state space allows for the exact numerical calculation of $\|X_p - G_p\|$ for small p, thus the spectral gap in the thermodynamic limit has the sharper lower bound based on Eq. (A.4) in Appendix A.1:

$$\epsilon \geq \frac{\epsilon_{2p}}{2}\left(1-\sqrt{2}\left(\|X_p - G_p\| \cdot (\|X_p\| + 2) + \delta_p \|X_p\|^2\right)\right)^2, \tag{5.27}$$

where δ_p is given by Eq. (5.22). Since the matrices X_p and $X_p - G_p$ are not sparse, this optimization is not applicable for the case $l = 9$. However, for $p = 5$ the bounds are improved in the regions where they are close to zero. The comparison of the improved martingale bounds with the Knabe bound is shown in Fig. 5.3. From around the point $r \approx 1.72$, the $l = 9$-martingale bound is the largest, so that region of the plot is analogous to Fig. 5.2b.

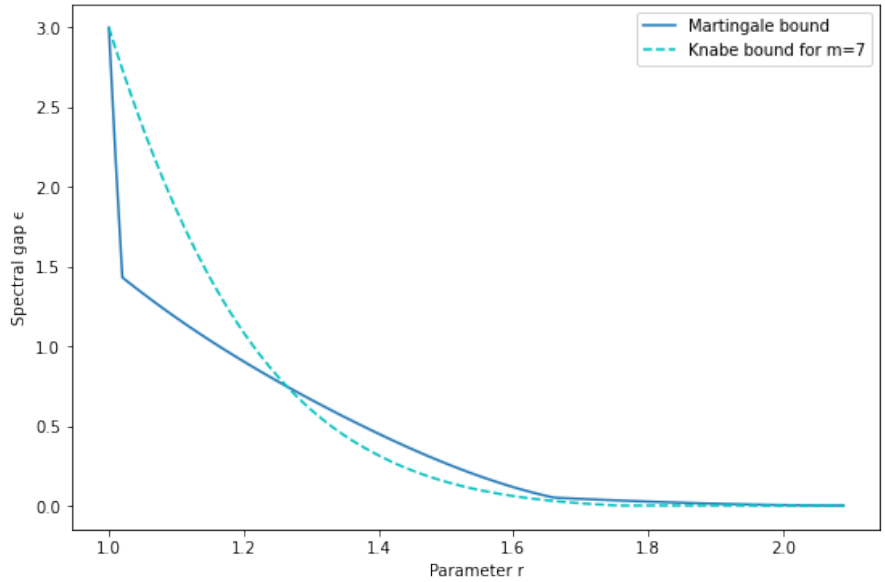

(a) Comparison in the range $1 \leq r \leq 2.1$

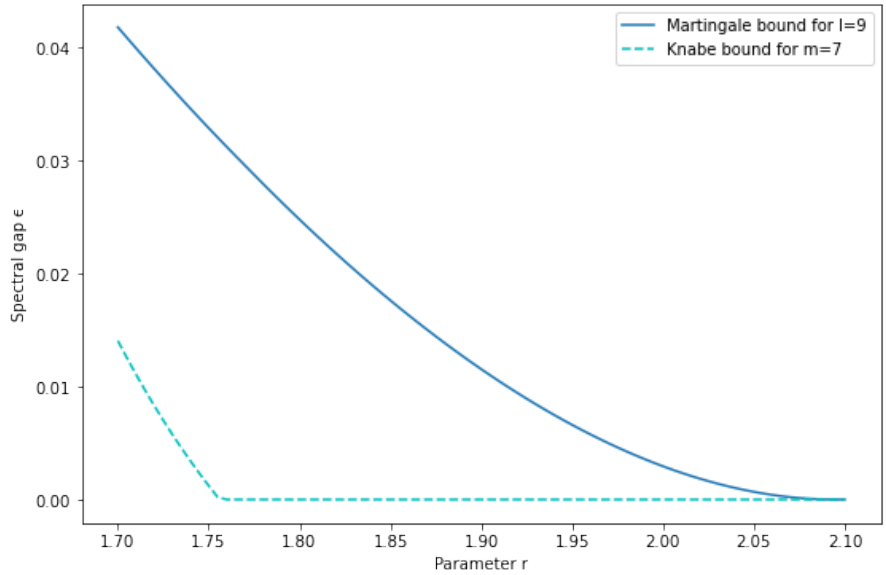

(b) Comparison in the range $1.7 \leq r \leq 2.1$ for $l = 9$

Figure 5.2.: Comparison of the Knabe and the mixed martingale bound for the deformed $\mathbb{Z}_3$-XY model

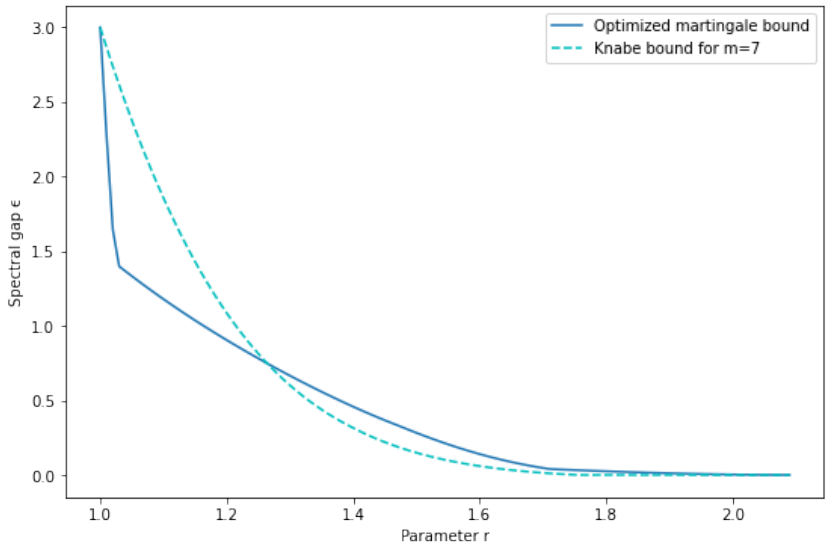

Figure 5.3.: Comparison of the Knabe and the optimized martingale bound for the deformed $\mathbb{Z}_3$-XY model

To summarize the obtained results, by using the martingale method the model is proven to be gapped in the whole parameter range $0 < r < \infty$ by the means of Eq. (5.25). Furthermore, bounds on the gap were calculated, where an optimized method provided better estimates in regions where the deformations are sufficiently large.

$\mathbb{Z}_3$-ANNNP model

For a more general outlook, the authors also considered a deformation

$$m_j = \begin{pmatrix} 1 & & \\ & r & \\ & & s \end{pmatrix}, \tag{5.28}$$

where r and s are real positive parameters. Since the gap calculations in [18] use Knabe's method, the estimates depend only on the orthogonal projections onto the spaces that are spanned by the individual ground states, it is sufficient to only give the matrices m_j that deform the ground states. Even though these conclusions do not depend on the choice of $C_{j,j+1}$, a ground state gap of any deformed clock model Hamiltonian can be bounded by the product of its second smallest eigenvalue and the gap obtained for the parent Hamiltonian. For the case $s = r$ there exists a non-trivial choice of $C_{j,j+1}$ which recreates a model introduced by Mahyaeh and Ardonne [36]:

$$C_{j,j+1} = K_j K_{j+1}, \quad \text{where } K_j = \mathbb{1} \otimes \cdots \otimes \mathbb{1} \otimes k_j \otimes \mathbb{1} \otimes \cdots \otimes \mathbb{1}, \quad \text{and } k_j = \operatorname{diag}(r, 1, r^{-1}). \tag{5.29}$$

The exact Hamiltonian obtained by this deformation is the following:

$$\tilde{H}_{j,j+1} = \epsilon - \left[\sigma_j \sigma_{j+1}^\dagger + \frac{f}{2}(\tau_j + \tau_{j+1}) + g_1 \tau_j \tau_{j+1} + g_2 \tau_j \tau_{j+1}^\dagger + \text{h.c.}\right], \tag{5.30}$$

where the parameters are given by

$$\begin{aligned} f &= \frac{2(2r+1)(1-r^3)}{9r^2} \qquad \epsilon = \frac{2(1+r+r^2)^2}{9r^2}, \\ g_1 &= -\frac{2(1-r)^2(1+r+r^2)}{9r^2}, \qquad g_2 = \frac{(1-r)^2(1-2r-2r^2}{9r^2}). \end{aligned} \tag{5.31}$$

The model is regarded as the generalization of the axial next-nearest neighbor Ising model, and is called the $\mathbb{Z}_3$-axial next-nearest neigbor Potts (ANNNP) model [18, 37]. For this specific model the spectral gap was found to be finite at least for $0.3483 \lesssim r \lesssim 3.9912$ in [18], where the best bounds for small values of r were obtained by considering a subsystem size $m = 3$.

The ground state degeneracy and the overlap structure of the model is the same as of the $\mathbb{Z}_3$-XY model, so δ_p has the same form as given in Eq. (5.22) with the overlaps

$$o^p(r) = \left(\frac{|r^2-1|}{1+2r^2}\right)^p. \tag{5.32}$$

Similarly, in order to prove the existence of a ground state gap for a given r, one just needs to find an integer p that solves the inequality

$$\left(\frac{|r^2-1|}{1+2r^2}\right)^p < \frac{1}{4}\left(1-\sqrt{2-\sqrt{2}}\right). \tag{5.33}$$

Due to the form of the overlap functions $o^p(r)$, the Hamiltonian given in Eq. (5.30) is gapped in the whole parameter range $0 < r < \infty$. Equivalently, we can find an integer l that solves the inequality

$$\left(\frac{|r^2-1|}{1+2r^2}\right)^l < \frac{1}{4} - \frac{\sqrt{l+1}}{4\sqrt{l+1+\sqrt{l+1}}} \tag{5.34}$$

to arrive at the same conclusion. Even choosing a relatively small p in Eq. (5.33) extends the interval of r significantly where a nonzero estimate for spectral gap is obtained in comparison to the finite-size criteria in [18]: for $p = 5$, an estimate for the spectral gap can be obtained for any $0.4504 \lesssim r < \infty$. However, a relatively large p is required to find estimates for the spectral gap for $r \lesssim 0.3483$: by directly solving Eq. (5.33), we find that the choice $p \geq 9$ (or $l \geq 11$ by Eq. (5.34)) is necessary to detect bounds in that region, which requires significantly more computational time than the exact diagonalization of the 3-body Hamiltonian for the Knabe bound [18].

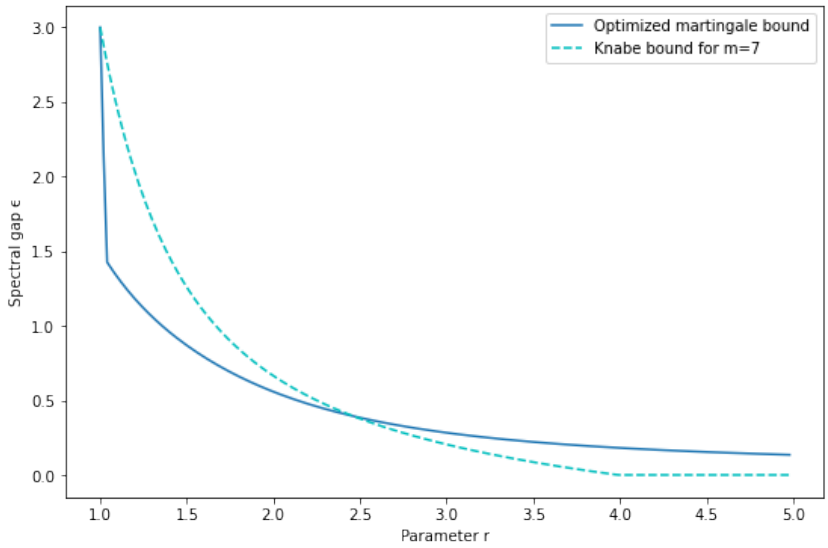

Figure 5.4.: Comparison of the Knabe and the optimized martingale bounds for the deformed $\mathbb{Z}_3$-ANNNP model

The martingale method optimized for such clock models achieved an improved bound on the spectral gap in the parameter region $2.461 \lesssim r$. In Fig. 5.4 the optimized martingale bounds (for $p = 5$ or $l = 1$) and the Knabe bounds are shown in the parameter range $1 \leq r \leq 5$.

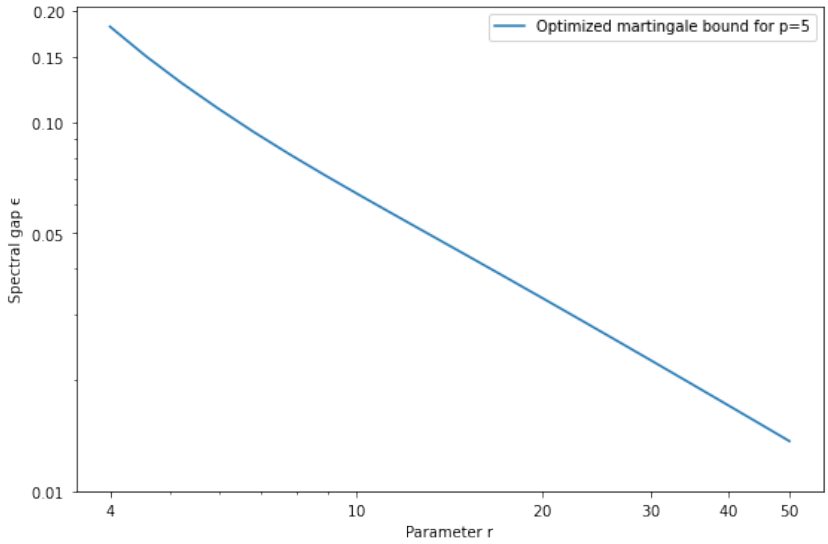

Figure 5.5.: Log-log plot of the martingale bound for the deformed $\mathbb{Z}_3$-ANNNP model

Since the martingale method provides a gap estimate for larger values of r, the obtained

results for the range $4 \leq r \leq 50$ are shown in Fig. 5.5 in the form of a log-log plot.

5.2.2. $\mathbb{Z}_4$-ANNNP model

Now, we consider a system which has a 4-fold degenerate ground space. The deformations are given as

$$m_j = \mathrm{diag}\,(1, r, r^2, r), \qquad k_j = \mathrm{diag}\,(r, r, r^{-1}, r^{-1}). \tag{5.35}$$

Consequently, the local Hamiltonian is of the form

$$\tilde{H}_{j,j+1} = \epsilon - \left(\sigma_j \sigma_{j+1}^\dagger + \frac{f}{2}(\tau_j + \tau_{j+1}) - U \tau_j \tau_{j+1} + \mathrm{h.c.} \right), \tag{5.36}$$

where the σ and τ matrices now satisfy the relations given in Eq. (5.5) for $d = 4$, and the parameters of the Hamiltonian are given as

$$f = \frac{r^{-2} - r^2}{2}, \quad U = \frac{(r - r^{-1})^2}{4}, \quad \epsilon = \frac{(r + r^{-1})^2}{2}. \tag{5.37}$$

In [18] the authors concluded that due to the local gap of the 3-body Hamiltonian

$$\epsilon_3 = \frac{1}{2} + \frac{\min\,(r^2, r^{-2})}{r^2 + r^{-2}}, \tag{5.38}$$

Knabe's method detects the gap in the whole parameter range $0 < r < \infty$ and provides an explicit expression of the bound which is then

$$\tilde{\epsilon} \geq \frac{4 \min\,(r^2, r^{-2})}{r^2 + r^{-2}}. \tag{5.39}$$

The martingale-type argument also proves that the model is gapped in the whole parameter range: by utilizing Eq. (4.63) (and Eq. (4.33) to see that the left-hand side of Eq. (4.63) is bounded from above by γ_p) for any Witten conjugated clock model we have

$$\gamma_p \leq \frac{1}{(1 - 6 o_{\max}^{(p)})^2} - 1. \tag{5.40}$$

Now we calculate the largest overlap $o_{\max}^{(p)}$ of the ground spaces

$$o_{\max}^{(1)} = \frac{|r^2 - 1|}{(r^2 + 1)}, \qquad o_{\max}^{(p)} = \left(o_{\max}^{(1)} \right)^p. \tag{5.41}$$

Along with the condition $\gamma_p < 1/\sqrt{2}$ we arrive to the inequality

$$\left(\frac{1}{1-6\left(\frac{|r^2-1|}{r^2+1}\right)^p}\right)^2 < 1+\frac{1}{\sqrt{2}}. \tag{5.42}$$

For any $0 < r < \infty$ there exists a $p \in \mathbb{N}$ such that this inequality holds, thus the Hamiltonian is gapped in the whole parameter range.

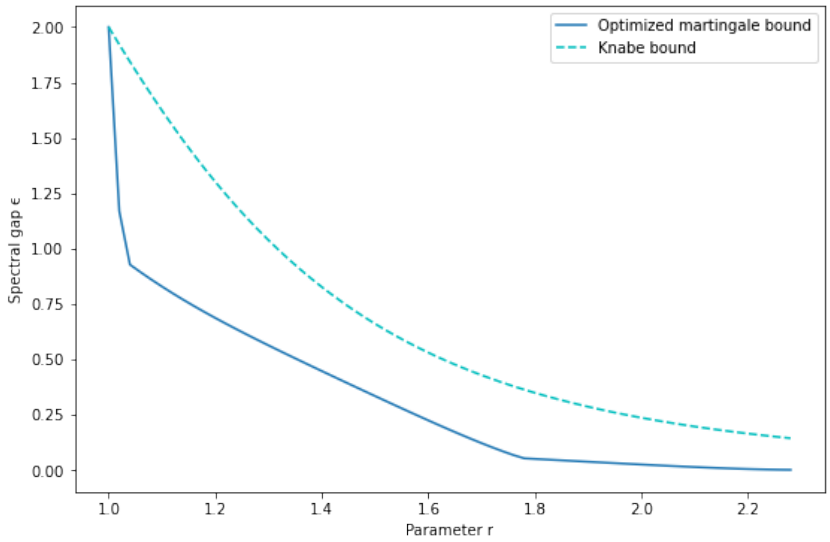

Figure 5.6.: Comparison of the Knabe and the martingale bounds for the deformed $\mathbb{Z}_4$-ANNNP model

In contrast to Knabe's method, the martingale method only provides numerical estimates for the gap in limited intervals.

The plots for $1 \leq r \leq 2$ are shown in Fig. 5.6, where the martingale bound is calculated for $l = 1$, $l = 9$ and $p = 5$ in accordance with Eq. (5.26) and Eq. (5.24). The Hamiltonian is invariant under the transformation $r \mapsto 1/r$, so the results follow analogously for $r < 1$. Furthermore, for the choice $l = 9$ the martingale method provides a bound for the spectral gap in the interval $0.4355 \lesssim r \lesssim 2.2964$.

6. Discussion

6.1. Summary

C*-finitely correlated states and matrix product states are both extremely important classes of states that characterize quantum spin chain systems. In this thesis, these two classes of states were introduced while highlighting their relations in a systematic manner. Most importantly, purely generated C*-finitely correlated states have a translation invariant MPS representation, and pure C*-finitely correlated states possess the properties of injective matrix product states. Furthermore, given an injective MPS, one can construct a frustration-free local Hamiltonian, called the parent Hamiltonian, which has a unique ground state in the form of that injective MPS.

The characterization of these classes of states was followed by the introduction of two well-established methods for bounding the spectral gap of frustration-free local Hamiltonians. Knabe's method requires Hamiltonians that are sums of nearest-neighbor orthogonal projections, and relates the spectral gap to the second smallest eigenvalue of the Hamiltonian taken on a smaller subsystem. If the local gap is larger than a certain threshold, then the Hamiltonian has a nonzero spectral gap in the thermodynamic limit. On the other hand, the martingale method only uses the local gap as a prefactor, thus its magnitude does not influence the conclusion about the existence of the spectral gap of the infinite system. In particular, the relevant condition relies on the structure of the ground state spaces.

In the case of the parent Hamiltonian of an injective MPS, the proof of [10, Lemma 6.2] was simplified and was made more accessible with the utilization of tensor network notation. The statement was then extended to Hamiltonians which have a finite number of ground states, all of which are of the form of an injective MPS in the thermodynamic limit. In that case, the bound on the spectral gap also depends on the overlap of the spaces spanned by the individual ground states. For the spectral gap estimate, which depends on the largest overlap between any two ground spaces, a missing factor was identified in comparison to [28, Prop. 12].

The main result of this thesis is the comparison of Knabe's method and the martingale method for clock models that are deformed by the terms of Witten's conjugation. The ground state degeneracy of these models remain invariant under the deformation, and the ground states can be represented by an injective MPS. The utilization of the martingale method proved that all of the deformed clock models introduced in this thesis have a nonvanishing spectral gap in the thermodynamic limit for the whole parameter range where those models are defined. In that regard, the martingale method is more powerful than Knabe's method, which proved the existence of the spectral gap in limited intervals

in the parameter space, with the only exception being the $\mathbb{Z}_4$-ANNNP model.

The numerical results of the thesis provide a comparison of the spectral gap estimates produced by the two methods. These results imply that for the $\mathbb{Z}_3$ models the martingale method provides a better estimate for the bound when the ground state overlaps are larger, i.e., when the deformations are stronger. Both methods require the second smallest eigenvalue of a finite-size Hamiltonian. In the case of the $\mathbb{Z}_3$ models, where the Knabe method did not provide an explicit expression for the gap estimate, the martingale method extended the region where a bound on the gap was found. By exploiting the sparsity of the Hamiltonians of these models, larger subsystem sizes were feasible with methods based on the Lánczos-algorithm. In contrast to that, Knabe's method requires projectors, that are not sparse in general. Due to the simplicity of the ground state spaces of these models, the martingale bounds were slightly improved by using non-approximated terms that were used to derive the expression for the bound. However, there still exist parameter intervals in these models, where the Knabe bounds outperform the martingale bounds, independent of the subsystem size chosen for the martingale bound: a straightforward reasoning is the rescaling factor, which is smaller than one, that appears in the expression provided by the martingale method.

In the case of the $\mathbb{Z}_4$-ANNNP model, both methods proved that the Hamiltonian is gapped in the whole parameter range. However, Knabe's method provided a larger, analytically closed estimate for the spectral gap.

6.2. Outlook

The analysis provided in the thesis is by no means exhaustive. It is possible to enlarge the region where an explicit bound on the gap is obtained by increasing the system size and further optimize Lánczos-based methods to diagonalize the finite-size Hamiltonian associated with the finite length provided in the expression for the martingale bound. It would be furthermore possible to tailor Knabe's finite-size criterion to the actual Hamiltonian of the models given above, not the Hamiltonians constructed from the orthogonal complement of the ground state projectors. Thus, the two methods could be compared through the diagonalization of the same Hamiltonian on a larger subsystem. However, this approach might result in a less powerful or in a more tedious approximation, since the local Hamiltonian terms are not idempotent in general. One can also utilize more recent finite-size methods which again use projector Hamiltonians, and provide an improved local gap threshold e.g. the criterion provided in [38].

Another way of further exploration could be to test these methods for different classes of frustration-free models, e.g. some of the SU(n)-symmetric valence bound solids introduced in [39]. The MPS models given in that paper have a bond dimension larger than one, so the martingale bound will contain contributions from the second largest eigenvalue of the transfer matrices. However, these models require periodic boundary conditions, so the martingale method has to be modified along the lines of [40] to be applicable to those systems. In addition, it is necessary to rigorously prove that the states constructed in

[39] are the only ground states of their parent Hamiltonians in the thermodynamic limit, since this property has been mostly verified for finite system sizes only.

Since for the examples discussed in this thesis, the Hamiltonians remained gapped throughout the deformation, it would be intriguing to see whether Witten's conjugation can also somehow deform the phase diagram of frustration-free systems, that undergo a phase transition in their parameter space. A strategy to engineer such models is provided in [41] along with an example with nearest neighbor interactions.

Bibliography

[1] H. Bethe, "Zur Theorie der Metalle," *Zeitschrift für Physik*, vol. 71, no. 3, pp. 205–226, Mar. 1931.

[2] C. N. Yang, "Some exact results for the many-body problem in one dimension with repulsive delta-function interaction," *Phys. Rev. Lett.*, vol. 19, pp. 1312–1315, Dec 1967. [Online]. Available: https://link.aps.org/doi/10.1103/PhysRevLett.19.1312

[3] R. J. Baxter, "Exactly Solved Models in Statistical Mechanics," in *Integrable Systems In Statistical Mechanics*, G. M. D'Ariano, A. Montorsi, and M. G. Rasetti, Eds., 1985, pp. 5–63.

[4] F. Haldane, "Continuum dynamics of the 1-D heisenberg antiferromagnet: Identification with the O(3) nonlinear sigma model," *Physics Letters A*, vol. 93, no. 9, pp. 464–468, 1983. [Online]. Available: https://www.sciencedirect.com/science/article/pii/037596018390631X

[5] F. D. M. Haldane, "Nonlinear field theory of large-spin Heisenberg antiferromagnets: Semiclassically quantized solitons of the one-dimensional easy-axis Néel state," *Phys. Rev. Lett.*, vol. 50, pp. 1153–1156, Apr 1983. [Online]. Available: https://link.aps.org/doi/10.1103/PhysRevLett.50.1153

[6] E. Lieb, T. Schultz, and D. Mattis, "Two soluble models of an antiferromagnetic chain," *Annals of Physics*, vol. 16, no. 3, pp. 407–466, 1961. [Online]. Available: https://www.sciencedirect.com/science/article/pii/0003491661901154

[7] H. Tasaki, *Physics and Mathematics of Quantum Many-Body Systems*. Springer Cham, 2020.

[8] I. Affleck, T. Kennedy, E. H. Lieb, and H. Tasaki, "Valence bond ground states in isotropic quantum antiferromagnets," *Communications in Mathematical Physics*, vol. 115, no. 3, pp. 477–528, Sep. 1988.

[9] S. Knabe, "Energy gaps and elementary excitations for certain VBS-quantum antiferromagnets," *J Stat Phys*, vol. 52, 1988.

[10] M. Fannes, B. Nachtergaele, and R. Werner, "Finitely correlated states on quantum spin chains," *Communications in Mathematical Physics*, vol. 144, pp. 443–490, 1992.

[11] D. Perez-Garcia, F. Verstraete, M. M. Wolf, and J. I. Cirac, "Matrix product state representations," 2007.

[12] F. Verstraete and J. I. Cirac, "Matrix product states represent ground states faithfully," *Physical Review B*, vol. 73, no. 9, Mar. 2006. [Online]. Available: http://dx.doi.org/10.1103/PhysRevB.73.094423

[13] E. Lieb and D. Mattis, "Ordering energy levels of interacting spin systems," *Journal*

of Mathematical Physics, vol. 3, no. 4, pp. 749–751, 1962.

[14] W. Marshall, "Antiferromagnetism," *Proceedings of the Royal Society of London Series A*, vol. 232, no. 1188, pp. 48–68, Oct. 1955.

[15] A. Mazurenko, C. S. Chiu, G. Ji, M. F. Parsons, M. Kanász-Nagy, R. Schmidt, F. Grusdt, E. Demler, D. Greif, and M. Greiner, "A cold-atom fermi–hubbard antiferromagnet," *Nature*, vol. 545, no. 7655, p. 462–466, May 2017. [Online]. Available: http://dx.doi.org/10.1038/nature22362

[16] N. Schuch, D. Pérez-García, and I. Cirac, "Classifying quantum phases using matrix product states and projected entangled pair states," *Physical Review B*, vol. 84, no. 16, Oct. 2011. [Online]. Available: http://dx.doi.org/10.1103/PhysRevB.84.165139

[17] Z.-C. Gu and X.-G. Wen, "Tensor-entanglement-filtering renormalization approach and symmetry-protected topological order," *Physical Review B*, vol. 80, no. 15, Oct. 2009. [Online]. Available: http://dx.doi.org/10.1103/PhysRevB.80.155131

[18] J. Wouters, H. Katsura, and D. Schuricht, "Interrelations among frustration-free models via Witten's conjugation," *SciPost Physics Core*, vol. 4, 2021.

[19] J. C. Bridgeman and C. T. Chubb, "Hand-waving and interpretive dance: an introductory course on tensor networks," *Journal of Physics A: Mathematical and Theoretical*, vol. 50, no. 22, 2017. [Online]. Available: http://dx.doi.org/10.1088/1751-8121/aa6dc3

[20] J. Cirac, D. Pérez-García, N. Schuch, and F. Verstraete, "Matrix product density operators: *r*enormalization fixed points and boundary theories," *Annals of Physics*, vol. 378, p. 100–149, Mar. 2017. [Online]. Available: http://dx.doi.org/10.1016/j.aop.2016.12.030

[21] A. Molnar, Y. Ge, N. Schuch, and J. I. Cirac, "A generalization of the injectivity condition for projected entangled pair states," *Journal of Mathematical Physics*, vol. 59, no. 2, Feb. 2018. [Online]. Available: http://dx.doi.org/10.1063/1.5007017

[22] G. Vidal, "Efficient classical simulation of slightly entangled quantum computations," *Physical Review Letters*, vol. 91, no. 14, Oct. 2003. [Online]. Available: http://dx.doi.org/10.1103/PhysRevLett.91.147902

[23] G. Hörmann, "Lecture notes: C*-algebras with aspects of quantum physics," January 2024. [Online]. Available: https://www.mat.univie.ac.at/~gue/lehre/2324CStarQP/CAQP.pdf

[24] N. Schuch, I. Cirac, and D. Pérez-García, "PEPS as ground states: Degeneracy and topology," *Annals of Physics*, vol. 325, no. 10, p. 2153–2192, Oct. 2010. [Online]. Available: http://dx.doi.org/10.1016/j.aop.2010.05.008

[25] D. E. Evans and R. Høegh-Krohn, "Spectral properties of positive maps on C*-algebras," *Journal of the London Mathematical Society*, vol. s2-17, no. 2, pp. 345–355, 1978. [Online]. Available: https://londmathsoc.onlinelibrary.wiley.com/doi/abs/10.1112/jlms/s2-17.2.345

[26] M. Fannes, B. Nachtergaele, and R. Werner, "Finitely correlated pure states,"

Journal of Functional Analysis, vol. 120, no. 2, pp. 511–534, 1994. [Online]. Available: https://www.sciencedirect.com/science/article/pii/S002212368471041X

[27] M. Fannes, B. Nachtergaele, and R. F. Werner, "Abundance of translation invariant pure states on quantum spin chains," *Letters in Mathematical Physics*, vol. 25, no. 3, pp. 249–258, Jul. 1992.

[28] B. Nachtergaele, "The spectral gap for some spin chains with discrete symmetry breaking," *Communications in Mathematical Physics*, vol. 175, no. 3, p. 565–606, Feb. 1996. [Online]. Available: http://dx.doi.org/10.1007/BF02099509

[29] B. Nachtergaele, R. Sims, and A. Young, "Lieb-Robinson bounds, the spectral flow, and stability of the spectral gap for lattice fermion systems," *Mathematical Problems in Quantum Physics*, vol. 717, pp. 93–115, 2018.

[30] E. Witten, "Constraints on supersymmetry breaking," *Nuclear Physics B*, vol. 202, no. 2, pp. 253–316, 1982. [Online]. Available: https://www.sciencedirect.com/science/article/pii/0550321382900712

[31] A. Y. Kitaev, "Unpaired Majorana fermions in quantum wires," *Physics-Uspekhi*, vol. 44, no. 10S, p. 131, 2001. [Online]. Available: https://dx.doi.org/10.1070/1063-7869/44/10S/S29

[32] I. Peschel and V. J. Emery, "Calculation of spin correlations in two-dimensional Ising systems from one-dimensional kinetic models," *Zeitschrift für Physik B Condensed Matter*, vol. 43, p. 241, 1981. [Online]. Available: https://link.springer.com/content/pdf/10.1007/BF01297524.pdf

[33] W. Selke, "The ANNNI model — Theoretical analysis and experimental application," *Physics Reports*, vol. 170, no. 4, pp. 213–264, 1988. [Online]. Available: https://www.sciencedirect.com/science/article/pii/0370157388901408

[34] F. Iemini, C. Mora, and L. Mazza, "Topological phases of parafermions: A model with exactly solvable ground states," *Phys. Rev. Lett.*, vol. 118, p. 170402, Apr 2017. [Online]. Available: https://link.aps.org/doi/10.1103/PhysRevLett.118.170402

[35] R. Lehoucq, D. Sorensen, and C. Yang, *ARPACK Users' Guide: Solution of Large-scale Eigenvalue Problems with Implicitly Restarted Arnoldi Methods*, ser. Software, Environments, and Tools. Society for Industrial and Applied Mathematics, 1998. [Online]. Available: https://books.google.hu/books?id=iMUea23N_CQC

[36] I. Mahyaeh and E. Ardonne, "Exact results for a $\mathbb{z}_3$-clock-type model and some close relatives," *Phys. Rev. B*, vol. 98, p. 245104, Dec 2018. [Online]. Available: https://link.aps.org/doi/10.1103/PhysRevB.98.245104

[37] I. Peschel and T. T. Truong, "The kinetic Potts chain and related Potts models with competing interactions," *Journal of Statistical Physics*, vol. 45, no. 1, pp. 233–244, Oct. 1986.

[38] M. Lemm and E. Mozgunov, "Spectral gaps of frustration-free spin systems with boundary," *Journal of Mathematical Physics*, vol. 60, no. 5, p. 051901, 05 2019. [Online]. Available: https://doi.org/10.1063/1.5089773

[39] M. Greiter and S. Rachel, "Valence bond solids for SU(n) spin chains: Exact models, spinon confinement, and the Haldane gap," *Phys. Rev. B*, vol. 75, p. 184441, May 2007. [Online]. Available: https://link.aps.org/doi/10.1103/PhysRevB.75.184441

[40] A. M. Young, *Spectral properties of multi-dimensional quantum spin systems.* University of California, Davis, 2016.

[41] M. M. Wolf, G. Ortiz, F. Verstraete, and J. I. Cirac, "Quantum phase transitions in matrix product systems," *Physical Review Letters*, vol. 97, no. 11, Sep. 2006. [Online]. Available: http://dx.doi.org/10.1103/PhysRevLett.97.110403

A. Appendix

A.1. Proof sketch of the martingale bound for a degenerate ground state

This section sketches the proof of [28, Lemma 11.ii)] to bound γ_p from Eq. (4.33) for Hamiltonians, that have a finitely degenerate ground state, where all of the ground states are injective matrix product states. Some intermediate steps of the proof create the possibility of optimizing the method for simpler systems, where many of the quantities estimated throughout the proof can be computed explicitly. We start by using the triangle inequality:

$$\begin{aligned}\|G_{b+p+c} - (G_{b+p} \otimes \mathbb{1}_c)(\mathbb{1}_b \otimes G_{p+c})\| \leq & \| G_{b+p+c} - X_{b+p+c}\| \\ & + \left\| \sum_{\alpha=1}^{n} G^{\alpha}_{b+p+c} - (G^{\alpha}_{b+p} \otimes \mathbb{1}_c)(\mathbb{1}_b \otimes G^{\alpha}_{p+c}) \right\| \\ & + \left\| \left(\sum_{\alpha=1}^{n} (G^{\alpha}_{b+p} \otimes \mathbb{1}_c)(\mathbb{1}_b \otimes G^{\alpha}_{p+c}) \right) - (G_{b+p} \otimes \mathbb{1}_c)(\mathbb{1}_b \otimes G_{p+c}) \right\|, \end{aligned} \tag{A.1}$$

where $X_p = \sum_{\alpha=1}^{n} G^{\alpha}_p$. Eq. (4.60) provides a bound on the first term, and a repeated use of the triangle inequality and then Eq. (4.56) upper bounds the second term. Since we can write

$$\sum_{\alpha=1}^{n} (G^{\alpha}_{b+p} \otimes \mathbb{1}_c)(\mathbb{1}_b \otimes G^{\alpha}_{p+c}) = (X_{b+p} \otimes \mathbb{1}_c)\,(\mathbb{1}_b \otimes X_{p+c}) - \sum_{\alpha \neq \beta} (G^{\alpha}_{b+p} \otimes \mathbb{1}_c)(\mathbb{1}_b \otimes G^{\beta}_{p+c}), \tag{A.2}$$

the third expression in the right hand side of Eq. (A.1) is bounded from above by

$$\begin{aligned} & \left\| \left(\sum_{\alpha=1}^{n} (G^{\alpha}_{b+p} \otimes \mathbb{1}_c)(\mathbb{1}_b \otimes G^{\alpha}_{p+c}) \right) - (G_{b+p} \otimes \mathbb{1}_c)(\mathbb{1}_b \otimes G_{p+c}) \right\| \\ & \qquad \leq \|(G_{b+p} \otimes \mathbb{1}_c)(\mathbb{1}_b \otimes G_{p+c}) - (X_{b+p} \otimes \mathbb{1}_c)\,(\mathbb{1}_b \otimes X_{p+c})\| \\ & \qquad + \left\| \sum_{\alpha \neq \beta} (G^{\alpha}_{b+p} \otimes \mathbb{1}_c)(\mathbb{1}_b \otimes G^{\beta}_{p+c}) \right\|. \end{aligned} \tag{A.3}$$

The first expression of the right hand side of Eq. (A.3) is estimated further:

$$\begin{aligned}
&\|(G_{b+p}\otimes\mathbb{1}_c)(\mathbb{1}_b\otimes G_{p+c}) - (X_{b+p}\otimes\mathbb{1}_c)\,(\mathbb{1}_b\otimes X_{p+c})\,\| \\
&\quad= \|(G_{b+p}\otimes\mathbb{1}_c)(\mathbb{1}_b\otimes G_{p+c}) - (G_{b+p}\otimes\mathbb{1}_c)(\mathbb{1}_b\otimes X_{p+c}) \\
&\qquad+ (G_{b+p}\otimes\mathbb{1}_c)(\mathbb{1}_b\otimes X_{p+c}) - (X_{b+p}\otimes\mathbb{1}_c)\,(\mathbb{1}_b\otimes X_{p+c})\,\| \\
&\quad\leq \|G_{b+p}\otimes\mathbb{1}_c\|\cdot\|\mathbb{1}_b\otimes(G_{p+c}-X_{p+c})\| \\
&\qquad+ \|(G_{b+p}-X_{b+p})\otimes\mathbb{1}_c\|\cdot\|\mathbb{1}_b\otimes X_{p+c}\| \\
&\quad= \|G_{p+c}-X_{p+c}\| + \|G_{b+p}-X_{b+p}\|\cdot\|X_{p+c}\| \\
&\quad\leq \frac{\delta_{p+c}}{1-\delta_{p+c}} + \frac{\delta_{b+p}}{1-\delta_{b+p}}\cdot\frac{1}{1-\delta_{p+c}}.
\end{aligned} \tag{A.4}$$

The last inequality used Eq. (4.60) explicitly for the norms of the form $\|X_p - G_p\|$, and the proof of that bound provided a bound for the norm $\|X_{p+c}\|$ as well. To avoid the dependency on the boundaries, we utilize the monotonicity of δ_p to arrive at the bound

$$\|(G_{b+p}\otimes\mathbb{1}_c)(\mathbb{1}_b\otimes G_{p+c}) - (X_{b+p}\otimes\mathbb{1}_c)\,(\mathbb{1}_b\otimes X_{p+c})\,\| \leq \left(1+\frac{1}{1-\delta_p}\right)\frac{\delta_p}{1-\delta_p}. \tag{A.5}$$

The second term in the expression Eq. (A.3) is bounded through a similar argument that was given in the proof for the existence of the spectral gap for a Hamiltonian, that has an injective MPS as a unique ground state. Together with a technical detail [28, Eq. (6.7)] that relates the sum of inner products of distinct ground state vectors to δ_p and the norm of the sum of those vectors individually, we arrive at

$$\|\sum_{\alpha\neq\beta}(G^{\alpha}_{b+p}\otimes\mathbb{1}_c)(\mathbb{1}_b\otimes G^{\beta}_{p+c})\| \leq \delta_p\|X_p\|^2 \leq \frac{\delta_p}{(1-\delta_p)^2}. \tag{A.6}$$

By summing up all of the obtained bounds we arrive at

$$\|G_{b+p+c} - (G_{b+p}\otimes\mathbb{1}_c)(\mathbb{1}_b\otimes G_{p+c})\| \leq \frac{2\delta_p}{1-\delta_p} + \frac{2\delta_p}{(1-\delta_p)^2} + \sum_{\alpha=1}^{n} D_\alpha^2\lambda_\alpha^p\,\frac{1+D_\alpha^2\lambda_\alpha^p}{1-D_\alpha^2\lambda_\alpha^p}, \tag{A.7}$$

and since $1/(1-\delta_p) > 1$, we also have

$$\|G_{b+p+c} - (G_{b+p}\otimes\mathbb{1}_c)(\mathbb{1}_b\otimes G_{p+c})\| \leq \frac{4\delta_p}{(1-\delta_p)^2} + \sum_{\alpha=1}^{n} D_\alpha^2\lambda_\alpha^p\,\frac{1+D_\alpha^2\lambda_\alpha^p}{1-D_\alpha^2\lambda_\alpha^p}. \tag{A.8}$$